Novel alkenone-producing strains of genus *Isochrysis* (Haptophyta) isolated from Canadian saline lakes show temperature sensitivity of alkenones and alkenoates

Hiroya Araie[a,b†], Hideto Nakamura[c,d,e†], Jaime L. Toney[f], Heather A. Haig[g], Julien Plancq[f], Takashi Shiratori[a], Peter R. Leavitt[g,h], Osamu Seki[d,i], Ken-ichiro Ishida[a], Ken Sawada[c,d], Iwane Suzuki[a,b], Yoshihiro Shiraiwa[a,b*]

[a] Faculty of Life and Environmental Sciences, University of Tsukuba, Tsukuba, 305-8572, Japan

[b] CREST, Japan Science and Technology Agency (JST), Tsukuba, 305-8572, Japan

[c] Department of Earth and Planetary Sciences, Faculty of Science, Hokkaido University, Sapporo, 060-0810, Japan

[d] CREST, Japan Science and Technology Agency (JST), Sapporo, 060-0810, Japan

[e] Department of Geosciences, Osaka City University, Osaka, 558-8585, Japan (present address of HN)

[f] School of Geographical and Earth Sciences, University of Glasgow, Glasgow, G12 8QQ, UK

[g] Limnology Laboratory, Department of Biology, University of Regina,

Regina, Saskatchewan, S4S 0A2, Canada

[h] Institute of Environmental Change and Society, Faculty of Science, University of Regina, Regina, Saskatchewan, S4S 0A2, Canada

[i] Institute of Low Temperature Science, Hokkaido University, Sapporo, 060-0814, Japan

[f] Equal contribution

*Corresponding author. Tel.: +81-29-853-4668. E-mail address: emilhux@biol.tsukuba.ac.jp (Y. Shiraiwa).

Abbreviations: LCAs, long chain alkenones; LSU, Rubisco large subunit; Rubisco, ribulose bisphosphate carboxylase/oxygenase; SST, sea surface temperature; SSU, Rubisco small subunit; U_{37}^{A}, U_{38}^{A}, RIA_{38} and A_{37}/A_{38} ,alkenoate indices; U_{37}^{K}, $U_{37}^{K'}$, $U_{37}^{K''}$, U_{38}^{K}Et, U_{41}^{K}Me and U_{42}^{K}Et, alkenone unsaturation indices.

Abstract

Alkenone-producing species have been recently found in diverse lacustrine environments, albeit with taxonomic information derived indirectly from environmental genomic techniques. In this study, we isolated alkenone-producing algal species from Canadian saline lakes and established unialgal cultures of individual strains to identify their taxonomical and molecular biological characteristics. Water and sediments collected from the lakes were first enriched in artificial seawater medium over a range of salinities (5–40‰) to cultivate taxa *in vitro*. Unialgal cultures of seven haptophyte strains were isolated and categorized in the *Isochrysis* clade using SSU and LSU rRNA gene analysis. The alkenone distributions within isolated strains were determined to be novel compared with other previously-reported alkenone-producing haptophytes. While all strains produced the typical C_{37} and C_{38} range of isomers, one strain isolated from Canadian salt lakes also produced novel C_{41} and C_{42} alkenones that are temperature sensitive. In addition, we showed that all alkenone unsaturation indices (e.g., U_{37}^{K} and $U_{37}^{K\prime}$) are temperature dependent in culture experiments, and that alkenoate indices (e.g., U_{37}^{A}, U_{38}^{A}, RIA_{38} and A_{37}/A_{38}) provide alternative options for temperature calibration based on these new lacustrine algal strains. Importantly, these indices show temperature dependence in culture experiments at temperatures below

10 ˚C, where traditional alkenone proxies were not as sensitive. We hypothesize that this suite of calibrations may be used for reconstructions of past water temperature in a broad range of lakes in the Canadian prairies.

Keywords: Alkenoates, Alkenones, Alkenone unsaturation index, Canadian salt lakes, Chemotaxonomy, Haptophytes, *Isochrysis*, Long-chain alkyl ketones, Paleothermometer, U^{K}_{37}

1. Introduction

Long-chain alkenones (LCAs) were originally reported in the marine sediments ca. 35 years ago (Boon et al., 1978; Brassell et al., 1980; de Leeuw et al., 1980; Volkman et al., 1980a, b; Marlowe et al., 1984) and in Quaternary lacustrine sediments a few years later (Cranwell, 1985; Volkman et al., 1988). Typically these LCAs exhibit chain lengths from C_{35} to C_{40} and contain 2–4 *trans*-type carbon double bonds, with C_{37}–C_{39} LCAs appearing as the most common chain lengths in previous literature. The marine coccolithophore, *Emiliania huxleyi*, was the first haptophyte identified to have produced LCAs (Volkman et al., 1980a, b). These algae have been widely studied, in part because haptophytes change the proportion of alkenones having a different number of double bonds depending on growth temperature. Consequently, the ratio of LCAs with different unsaturation levels is now used to calculate indices, such as U_{37}^{K} and $U_{37}^{K\prime}$, that can be used as paleotemperature proxies to reconstruct past sea surface temperature (SST) (Brassell et al., 1986; Prahl and Wakeham, 1987; Brassell, 1993).

Only five species within the Order Isochrysidales, Phylum Haptophyta are reported to produce LCAs and analogous compounds such as alkyl alkenoates (Medlin et al. 2008). Although LCAs are now found frequently in saline and freshwater inland lakes (e.g., Pearson et al., 2008; Theroux et al., 2010; Toney et al., 2010; D'Andrea et al., 2011;

90 Toney et al. 2012; Longo et al., 2013), it appears that these compounds
91 are still constrained to the Phylum Haptophyta. At present, taxa
92 known to produce alkenones fit into three taxonomical groups as
93 defined by Theroux et al. (2010). Group III includes *Emiliania huxleyi*
94 and *Gephyrocapsa oceanica* (Family Noelaerhabdaceae), which are
95 characteristic of marine environments. Group II includes *Isochrysis*
96 *galbana*, *Tisochrysis lutea* (Bendif et al., 2013), *Ruttnera lamellosa*
97 (revised from *Chrysotila lamellosa*; Andersen et al., 2014), which
98 belong to Family Isochrysidaceae and represent species found in a wide
99 range of environments such as coastal regions, brackish waters and
100 saline lakes. Group I is composed of haptophytes from which no living
101 algal strains have been isolated, but for which putative haptophyte
102 strains have been identified by using environmental genomics of
103 Rubisco small subunit (SSU) rRNA from environmental samples
104 collected in freshwater environments (D'Andrea et al., 2006; Theroux
105 et al., 2010; Longo et al., 2013, 2016).

106 Freshwater alkenone-producing haptophytes have gained
107 interest of the paleoclimate community because of the potential for
108 their LCAs as indices of past continental climates (Zink et al., 2001;
109 Chu et al., 2005, 2012; Hou et al., 2016). However, the use of these
110 compounds has been constrained to date because specific LCA-
111 producing strains have not been isolated from the source lakes, and

112 little is known of the environmental preferences of producer
113 populations. Analysis of environmental SSU rRNA suggests that
114 several alkenone-producing haptophyte species closely related to
115 *Isochrysis* and/or *Ruttnera* (Family Isochrysidaceae) live in saline lakes
116 and brackish waters where the LCAs are associated with organic
117 matter suspended in water and sediments (Coolen, 2004, Coolen et al.,
118 2009; Theroux et al., 2010; Toney et al., 2012, Randlett et al., 2014).
119 The most recent investigation of northern Alaskan lakes reveals that
120 those LCAs are characterized by abundant $C_{37:4}$ homologues forms and
121 a series of $C_{37:3}$ alkenone isomers. Furthermore, Longo et al. (2016)
122 used suspended particulate matter in Toolik Lake to determine an *in*
123 *situ* U^K_{37}-temperature calibration for that freshwater site. However,
124 despite these important advances, the absence of strain-specific
125 information on environmental preferences makes it difficult to
126 determine whether site-, habitat- and species-specific calibrations may
127 be required for haptophytes from non-marine settings. While alkenone-
128 derived, U^K_{37}-temperature calibrations have been developed for several
129 genetically distinct strains of haptophytes (Versteegh et al., 2001;
130 Rontani et al., 2004; Sun et al., 2007; Ono et al., 2012; Nakamura et al.,
131 2014, 2016; Zheng et al., 2016), isolates from additional environments
132 are still needed to determine the applicability of a universal calibration.

133 To date, existing U^K_{37}-temperature calibrations exhibit similar

134 relationships (slopes) to environmental temperature, suggesting a
135 similar dependence of unsaturation on temperature (Theroux et al.,
136 2010; Bendif et al., 2013; Nakamura et al., 2016). However, the y-
137 intercepts of U^K_{37}-temperature calibrations vary among indicator ratios
138 and may reflect the influence of other physiological, taxonomic or
139 environmental parameters. In addition, most LCA-based
140 paleotemperature reconstructions have been performed in
141 environments where diverse haptophyte species with distinctive LCA
142 composition are expected to co-occur, including Chesapeake Bay
143 (Schwab and Sachs, 2011), the Black Sea (Coolen et al., 2009), the
144 Nordic Sea (Bendle et al., 2005) and the Baltic Sea (Schulz et al., 2000),
145 making it difficult to determine whether reconstructions arise from
146 temperature–related shifts in saturation level or environmentally-
147 controlled changes in species composition. Consequently, further
148 detailed studies are needed on the thermal ecology of producing
149 organisms and on how LCA compositions may change through time
150 due to different control pathways (temperature, nutrient status, etc.) to
151 fully understand the controls on unsaturation dependence on
152 temperature.

153 In this study, we isolated and identified seven alkenone-
154 producing algae from Canadian saline lakes to better establish the
155 relationship between environmental conditions and LCA production.

Our new strains were grouped at unique phylogenic positions within the genus *Isochrysis*, including the first report of alkenone-producing *I. galbana* from inland lakes. The LCA compositions of some strains were different from those of marine *I. galbana,* which was reported by Theroux et al. (2013). Although the unsaturation dependence of the LCAs on temperature for the newly isolated *Isochrysis* strains was similar to those from unidentified alkenone-producing sedimentary isolates in a previous study (Toney et al., 2012), the y-intercept of new LCA ratios was different, suggesting an alternate control on the y-intercept of the U_{37}^{K} calibration. The addition of the multiple, phylogenetically-distinct *Isochrysis* strains enabled us to discuss the relationship between phylogeny and LCA composition, including that between the degree of compound unsaturation and environmental temperature for species within the genus *Isochrysis*.

2. Materials and methods

2.1 Location of Canadian lakes for isolating alkenone-producing microalgae

We selected ten Canadian saline lakes where LCAs were already detected by Toney et al. (2011) and environmental data were available from an earlier comprehensive survey (Pham et al. 2009). Lakes

Antelope, Snakehole, Success, Fishing, Humboldt, Waldsea, Deadmoose, Charron, Rabbit, and Redberry are saline lakes located in Saskatchewan, Canada (Supplementary Fig. S1, Table 1). In the present study, temperature, pH and salinity profiles were measured at 1-m depth intervals using a YSI Pro Plus meter (YSI Inc., Yellow Springs, Ohio, USA).

2.2 Isolation and establishment of alkenone-producing microalgal strains as unialgal culture

Samples of lake water, lake sediments, shore sand and plankton were collected with a 4-L Van-Dorn water sampler, Ekman grab, and plankton net (mesh pore size 5 µm), respectively, in September 2014. The samples were transported to the laboratory of the University of Regina, Regina, Canada, for the isolation of microalgae. The sample types (water, sediment, and plankton) were individually combined with a fresh culture medium for microalgae using either AF6 modified (prepared according to NIES-Culture Collection Media List, NIES, Japan, originally from Watanabe et al., 2000) or an artificial seawater (Marine Art SF-1; Osaka Yakken, Osaka, Japan) enriched with a modified Erd–Schreiber's medium containing 10 nM disodium selenite (MA-ESM as described in Danbara and Shiraiwa, 1999).

MA-ESM media was prepared with a range of salinities to match the salinity of each lake by adjusting the amount of Marine Art SF-1 powder to achieve salinities varying from 5 ‰ and 40 ‰. Then the medium was diluted using techniques for isolating single species of microalgae, as described by Allen and Stanier (1968). The algal suspension diluted with the fresh medium was dispensed into wells of a transparent, plastic, 96-well microplate. The salinity of the culture medium was set at 40, 30 or 10 ‰, as shown in Table 2. For the cultivation of microalgae, the plates were maintained in a plant growth chamber under illumination by 20W-fluorescent lamp with an intensity range of 28 to 43 µmol photons m^{-2} s^{-1} (range: 400–700 nm) with a 12-h light/12-h dark regime. The temperature in the chamber was kept constant at 10 °C during culture.

2.3 Culture of the established strains as unialgal culture for testing temperature effect

Algal strains isolated from Canadian lakes were individually established as unialgal cultures by using the dilution method, as described above. Those strains were grown in 50-mL plastic flasks containing the MA-ESM medium with various ranges of salinity from 10 to 40‰ (Table 2). All cultures were maintained in the algal growth chamber where light intensity and temperature were controlled. The

220 cultures were continuously illuminated by 20W-fluorescent lamps at
221 the intensity of 100 µmol photons m^{-2} s^{-1}. For testing temperature
222 effect, three representative strains were used. The temperature was
223 separately set at 5, 10, 15, 20 and 25 °C. Cells were grown until the
224 late linear or the early stationary growth phases when they were
225 harvested. Monitoring was achieved using the optical cell density of the
226 cell suspension. The culture periods were different among culture
227 vessels depending on growth rate in each culture and ranged from 16
228 days to 23 days. The harvested cells were used for the lipid analysis of
229 LCAs and alkenoates.

230

231 *2.4 DNA extraction, polymerase chain reaction (PCR) and sequencing*

232 After algal cells were harvested by centrifugation, DNA was
233 extracted from the cells using a DNeasy plant mini kit (Qiagen, Hilden,
234 Germany). The D1–D2 region of the large subunit (LSU) rRNA gene
235 was amplified by the PCR reaction using the haptophyte specific primer
236 set Hapto_4 (5'-ATGGCGAATGAAGCGGGC-3') and Euk_34r (5'-
237 GCATCGCCAGTTCTGCTTACC-3') (Liu et al., 2009). The
238 amplifications consisted of 30 cycles of denaturing at 98 °C for 10 s,
239 annealing at 55 °C for 15 s, and extension at 72 °C for 1 min by using
240 PrimeSTAR GXL DNA polymerase (Takara Bio, Ohtsu, Japan). The
241 SSU rRNA gene of isolates was amplified by the PCR reaction using

242 primer set 18F (5'-AACCTGGTTGATCCTGCCAG-3') and 18R (5'-
243 CYGCAGGTTCACCTACGGAA-3') (Yabuki et al., 2010). The
244 amplifications consisted of 30 cycles of denaturing at 98 °C for 10 s,
245 annealing at 55 °C for 15 s, and extension at 72 °C for 2 min by using
246 PrimeSTAR GXL DNA polymerase (Takara Bio). These amplified DNA
247 fragments were sub-cloned into *E. coli* strain JM109 and then
248 sequenced using a 3130 Genetic Analyzer (Applied Biosystems,
249 Waltham, MA, USA) with a BigDye Terminator v3.1 cycle sequencing
250 kit (Applied Biosystems).

251

252 *2.5 Sequence alignments and phylogeny*

253 For molecular phylogenic analysis, we newly created two
254 datasets of haptophyte; one is D1–D2 region of LSU rRNA gene
255 sequences, while the other is whole region of SSU rRNA gene
256 sequences. The datasets were automatically aligned with mafft-linsi
257 (Katoh and Standley, 2013), and then edited manually with SeaView
258 (Galtier et al., 1996). Ambiguously aligned regions were manually
259 deleted from the alignments. Finally, we prepared a LSU rRNA gene
260 alignment with 58 operational taxonomic units (OTUs) and 995
261 positions, and a SSU rRNA gene alignment with 100 OTUs and 1713
262 positions. The maximum likelihood (ML) tree was constructed using
263 IQ-TREE (Nguyen et al., 2015) under the best-fit model (TIM2+G4 for

LSU rRNA and TNe+G4 for SSU rRNA gene) determined by IQ-TREE. Non-parametric bootstrap analysis with 100 replicates was conducted under the best-fit models. The Bayesian analysis was performed on each alignment using MrBayes v. 3.2.2 (Ronquist et al. 2012) with the GTR +Γ model. Two separated Metropolis-coupled Markov chain Monte Carlo, each with one cold and three heated chains (default chain temperature = 0.1), were run for 5×10^6 generations. The lnL values and trees were sampled every 100 generation intervals. The convergence was assessed based on the average standard deviation of split frequencies, and the first 2×10^6 generations of each run were discarded as "burn-in." Bayesian posterior probability (BPP) and branch lengths were calculated from the remaining of the trees.

2.6 Lipid extraction and fractionation by organic solvents

The total lipid content of cells were extracted and separated into different compound classes for analysis using methods of Sawada et al. (1996) and Nakamura et al. (2014). Briefly the lipids were successively extracted from whole algal cells with methanol (MeOH), dichloromethane (DCM):MeOH (1:1 v:v) and DCM. The combined extracts were vigorously shaken after the addition of distilled water, and subsequently centrifuged to separate into two layers: lipid and water-soluble fractions. The resulting organic solvent layer was passed

286 through an anhydrous Na_2SO_4 column to remove water. The lipid
287 extract was dried in a rotary evaporator and subsequently re-dissolved
288 with *n*-hexane. The lipid-containing hexane extracts were separated
289 using a silica gel column into three fractions with *n*-hexane, *n*-
290 hexane:ethyl acetate (9:1, v:v) and ethyl acetate:MeOH (1:1, v:v) to
291 yield hydrocarbons, LCAs, and polar lipids (e.g., sterols and fatty acids),
292 respectively. After adding an internal standard (*n*-hexatriacontane),
293 those three fractions were analyzed by GC and GC–MS to quantify the
294 various compounds they contained.

295 The LCA fraction was further cleaned up by saponification to
296 reduce contamination from non-LCA compounds. Here a portion of the
297 alkenone fraction was saponified by heating at 70 °C for 3 h in 1 N
298 KOH MeOH:H_2O (95:5, v:v). After saponification, resultant products
299 were extracted three times with 1 ml each of *n*-hexane and
300 subsequently brought to the analysis of components using both GC and
301 GC–MS.

302 LCAs were also extracted from the lake sediments collected at
303 the Canadian sites. Briefly, freeze-dried sediments were homogenized
304 and extracted with DCM:MeOH (9:1, v:v) using a Dionex model
305 ASE350 accelerated solvent extractor. Following evaporation of the
306 solvent, the total lipid extracts were separated into neutral and acid
307 fractions by elution through a LC-NH_2 SPE column using

DCM:isopropyl alcohol (1:1, v:v) followed by ether with 4% acetic acid (v:v) as eluents, respectively. The neutral fractions were further separated into four fractions of increasing polarity by chromatography over a silica gel column packed with 35-70 μm particles using hexane, DCM, ethyl acetate:hexane (1:3, v:v) and MeOH as eluents. The second fractions (DCM fraction) containing LCAs were saponified using the same procedure as described above.

2.7 GC and GC–MS analyses

GC was conducted using a Shimadzu GC-2025 instrument equipped with FID for quantification of alkenone fractions. Two methods were applied with different columns and respective temperature programs: Agilent VF-200ms column (60 m × 0.25 mm × 0.10 μm), temperature program was 50 °C (1 min) to 255 °C at 20 °C/min, to 300 °C at 3 °C/min, and subsequently to 320 °C at 10 °C/min (held 10 min); Agilent CPSil5CB column (50 m × 0.32 mm × 0.12 μm), temperature program was 90 °C (2 min) to 255 °C at 40 °C/min, to 300 °C at 1 °C/min, and subsequently to 320 °C at 10 °C/min (held 10 min).

The use of the VF-200ms column was demonstrated by Longo et al. (2013) to significantly improve the separation for long-chain LCAs.

However, $C_{37:4}$ alkenone and $C_{36:2}$FAEE alkenoate co-eluted under these conditions, therefore the CPSil5CB column was used to separate both compounds clearly, quantify the ratio of $C_{37:4}$ to $C_{37:2}$ compounds, and calculate the abundances of $C_{37:4}$ and $C_{36:2}$FAEE (Nakamura et al., 2014). The LCAs and alkenoates were identified by Agilent 6890N GC instrument coupled to an Agilent 5975 inert XL MSD quadruple mass spectrometer (electron ionization: 70 eV; emission current: 350 µA; m/z 50–650). The VF-200ms column and the identical temperature program as for GC analysis were used for GC–MS analysis. Helium was the carrier gas in both GC and GC–MS.

The LCAs and alkenoates consist of di-, tri- and tetra-unsaturated homologues. Generally, di-unsaturated LCAs possess double-bonds at Δ^{14} and Δ^{21} positions ($\Delta^{14,21}$), tri-unsaturated LCAs have a third double bond at the Δ^{7} position ($\Delta^{7,14,21}$) and the tetra-unsaturated alkenone has a fourth double bond at Δ^{28} ($\Delta^{7,14,21,28}$) (Dillon et al., 2016; Longo et al., 2016; Zheng et al., 2017). By using a GC column lined with a VF-200ms column, isomers of tri-unsaturated LCAs and alkenoates exhibit doublet-like peaks consisting of a left-hand peak and a right-hand peak correspond to $\Delta^{7,14,21}$ (Δ^{7} isomer; isomer a) at $\Delta^{14,21,28}$ (Δ^{28} isomer; isomer b), respectively.

2.8 Temperature indices

The alkenone unsaturation indices (U^K_{37}, $U^{K'}_{37}$, $U^{K''}_{37}$, U^K_{38}Et, U^K_{41}Me and U^K_{42}Et), alkenoate unsaturation indices (U^A_{37} and U^A_{38}), methyl and ethyl alkenoate ratio (A_{37}/A_{38}), and the isomeric ratio of alkenoates (RIA_{38}) were all calculated based on biochemical profiles of Canadian algal samples raised under diverse temperature regimes. Refer to Nakamura et al. (2016) for original references of indices. Finally, RIA_{38} was determined as the isomeric ratio of alkenoates ($C_{36:3}$FAEE) according to the definition of RIK indices proposed by Longo et al. (2016), calculated by the following equation; RIA_{38} = $C_{36:3a}$FAEE / ($C_{36:3a}$FAEE + $C_{36:3b}$FAEE), where $C_{36:3a}$FAEE and $C_{36:3b}$FAEE are isomers.

3. Results

3.1 Haptophyte strains isolated from Canadian lakes

Haptophyte strains were isolated successfully from nearshore sand or sediments of three central Canadian lakes, specifically Lakes Snakehole, Success and Deadmoose (Table 1, Table 2A). All basins were saline lakes, and two exhibited a clearly-defined thermocline accompanied by changes in pH and salinity (Supplementary Fig. S2). In contrast, algal isolation was unsuccessful for samples obtained from lake water and plankton net samples, even though marker genes were

identified in some living algal samples and whole-water environmental samples of Lakes Snakehole, Success and Waldsea (Table 1).

Strains isolated from Lake Snakehole were named as Sh 1 and 2 (Fig. 1A, B), two from Lake Success were named as Sc 1 and 2 (Fig. 1C, D), and three from Lake Deadmoose named as Dm 1, 2 and 3 (Fig. 1E–G). DNA sequences of SSU and LSU rRNA were amplified from seven isolated haptophytes and algal mixture from environmental samples such as water, plankton net and sediment by using haptophyte-specific primers. The results of successful amplification are as shown in Table 2 with the Genebank accession numbers. DNA sequences obtained from environmental samples, the prefix E was added to the strain number (e.g., Sh E1). The LSU rRNA sequence data of the environment DNA sample from Lake Waldsea was coded Ws E1.

The phylogenic analysis showed that DNA sequences of the Canadian lake-isolates and algal mixture from environmental samples were composed of four groups, namely Group A including Sh E2, Sh 2, Sh 1 and Sh E1, Group B including Sc E2, Sc 1, Sc 2, Group C including Dm 2, Dm 3, Dm 1, Sc E1, Sc E3 and Group D including Ws E1. Group A from Lake Snakehole occupied a unique phylogenetic position in the *I. galbana* clade. This phylogenic position was suggested by both maximum likelihood tree analysis of SSU and LSU rRNA sequences of the Canadian haptophyte strains (Fig. 2, Fig. 3). Groups B

394 and C were included in the *I. galbana* clade. Ws E1 obtained from Lake
395 Waldsea suggested that the existence of *R. lamellosa* (Fig. 3). Overall,
396 unialgal strains isolated from Lakes Success and Deadmoose showed a
397 swimming ability driven by flagella under microscopic analysis;
398 whereas, that from Lake Snakehole did not (Supplementary Fig. S3).
399 This observation is also supported by determinations of the phylogenic
400 positions of Group A, B and C.

401

402 *3.2 Growth characteristics of the established Canadian lake*
403 *haptophytes strains*

404 Strains Sh 1, Sc 2 and Dm 2 showed similar temperature-
405 dependent growth patterns when cultured over a range from 5–25 °C
406 (Fig. 4). In all strains, the logarithmic growth phase ended within 100
407 h and then proceeded to the linear growth phase above 15 °C up to
408 25 °C. The optimum growth temperature was 25 °C for Sc 2 and 20 °C
409 for Sh 1 and Dm 2. Below 20 °C, the growth pattern of those three
410 strains was similar. Algal growth also showed a clear lag phase slowly
411 followed by the logarithmic growth phase with a low rate below 10 °C.

412 The strain Sh 1 showed the greatest preference for cold waters,
413 with a high growth rate at 5 °C and suppressed growth at 25 °C (Fig. 4).
414 The strain Sc 2 showed opposite trend to Sh 1, with low growth at low

415 temperatures and increased growth rates at high temperatures. The
416 strain Dm 2 showed intermediate properties. In addition to growth
417 parameters, some strains exhibited physiological or morphological
418 responses to changes in temperature. For example, the number of cells
419 swimming decreased below 10 °C in strains Sc 2 and Dm 2 (data not
420 shown), whereas the shape of some cells became more round than
421 oblong (Supplementary Fig. S3).

422

423 *3.3 LCAs and alkenoates in newly established Canadian lake*
424 *haptophyte strains*

425 All haptophyte strains (Table 2A) were analyzed for LCAs using
426 a GC–FID approach (Supplementary Fig. S4**)**. As there was minimal
427 variation in GC–FID profiles for samples obtained from individual
428 lakes, only one strain from each lake was presented as representative
429 of the composition of LCAs and alkenoates including derivatives (Fig. 5,
430 Supplementary Table S1**)**.

431 The profiles of LCAs and alkenoates of the Canadian lake
432 strains were characterized by the occurrence of major components such
433 as C_{37} methyl alkenones, C_{38} ethyl alkenones, and relatively minor
434 components such as C_{39} and C_{40} alkenones. Overall, these patterns
435 were similar to those already published from other Isochrysidaceae

strains (Rontani et al., 2004; Sun et al., 2007; Theroux et al., 2013; Nakamura et al., 2014, 2016; Zheng et al., 2016). Additionally, C_{38} methyl and C_{39} ethyl LCAs were also detected as minor alkenone components. Further, along with LCAs, C_{36} methyl alkenoates (C_{36}FAMEs) and C_{36} ethyl alkenoates (C_{36}FAEEs) were also detected as significant components in the non-saponified alkenone fractions (Fig. 5C).

Isomers of tri-unsaturated LCAs and alkenoates exhibited doublet-like peaks consisting of a left-hand peak and a right-hand peak that may correspond to $\Delta^{7,14,21}$ (Δ^{7} isomer; isomer a) at $\Delta^{14,21,28}$ (Δ^{28} isomer; isomer b), respectively (Fig. 5). Among the previously reported tri-unsaturated isomers of LCAs, only minor amounts of the Δ^{28} isomer of $C_{38:3}$ alkenone ($C_{38:3b}$Et in Fig. 5C; Supplementary Table S1) were identified in Canadian lake samples. However, the double bond positions are still considered tentative in our analysis, even though the identification of isomeric alkenones and alkenoates using DMDS treatment in Dillon et al. (2016) and Zheng et al. (2017) is a robust protocol.

There were also lake-specific characteristics in LCAs among strains grown at 20 °C. Specifically, Sh 1 was characterized by the production of extended LCAs that eluted after C_{40} LCAs in GC–FID analysis (peaks 23 to 26 in Fig. 5). Previously, similar peaks have been

458 reported as C_{41} methyl and C_{42} ethyl LCAs with two and three double
459 bonds in samples isolated from Chinese inland saline lakes (Zhao et al.,
460 2014). Peaks 23 to 26 were assigned as C_{41} methyl– and C_{42} ethyl-
461 alkenones by comparing elution patterns and mass spectra reported by
462 Zhao et al. (2014). $C_{41:3}$Me (peak 23) and $C_{41:2}$Me (peak 24) were
463 characterized by $M^{+\cdot}$ at m/z 584 and 586, respectively. Both compounds
464 exhibited $[M–18]^+$ ion, indicating a methyl ketone. $C_{42:3}$Et (peak 25) and
465 $C_{42:2}$Et (peak 26) exhibited $[M^{+\cdot}]$ (m/z 598 and 600, respectively) and
466 $[M–29]^+$ ion, indicating a ethyl ketone.

467 The sedimentary LCAs from Lakes Snakehole, Success and
468 Deadmoose showed similar LCA profiles to the cultured isolates with
469 some notable differences. For instance, only the Snakehole
470 sedimentary LCAs were characterized by the presence of $C_{41:3}$Et.
471 Meanwhile, the sedimentary LCA profiles showed consistently fewer
472 numbers of LCAs compared to the culture isolates; lacking $C_{36:3}$FAME,
473 $C_{36:2}$FAME, $C_{36:3b}$FAEE, $C_{38:3b}$Et, $C_{38:3}$Me, $C_{38:2}$Me, $C_{39:3}$Et, $C_{41:2}$Me,
474 $C_{42:3}$Et, and $C_{42:2}$Et. The Snakehole sedimentary LCA profiles also
475 lacked $C_{36:4}$FAME and $C_{36:4}$FAEE that were present in the culture
476 samples. The Success sedimentary LCA profile also lacked $C_{39:2}$Me,
477 $C_{40:3}$Et, and $C_{40:2}$Et that were present in the culture samples. The
478 Deadmoose sedimentary LCA profiles also lacked $C_{40:3}$Et, $C_{40:2}$Et that
479 were present in the culture samples. Of those "culture-only" LCAs, C_{38}

480 methyl-, C_{39} ethyl-, and above C_{40} alkenones were minor compounds in
481 culture isolates, so their lack in sedimentary LCA profiles might be due
482 to small amount of these compounds.

483

484 *3.4 Growth temperature-dependent changes in alkenone and alkenoate*
485 *compositions and the alkenone unsaturation index*

486 The unsaturation indices of C_{37}–C_{42} LCAs were established
487 using Canadian lake haptophyte strains of Sh 1, Sc 2 and Dm 2 (Table
488 3, Fig. 6, Supplementary Table S2). Importantly, U^K_{41}Me and U^K_{42}Et
489 were available only for Sh 1 strain, because only Sh 1 produces C_{41} and
490 C_{42} LCAs. Overall, all alkenone unsaturation indices increased above
491 10 °C, but were relatively invariant below that temperature. Such a
492 low-temperature plateau in alkenone unsaturation index values
493 between 5 and 10 °C is seen in other isolates (Conte et al., 1998;
494 Versteegh et al., 2001; Nakamura et al., 2014).

495 Similar to findings with the LCAs, alkenoate unsaturation
496 indices based on both methyl and ethyl alkenoates (U^A_{37} and U^A_{38},
497 respectively) increased linearly with incubation temperature, whereas,
498 RIA_{38} and A_{37}/A_{38} decreased with growth temperature from 10 °C to
499 25 °C (Table 3, Fig. 7, Supplementary Table S2). Comparison of linear
500 and second-order polynomial regressions of the alkenone and alkenoate

indices (10 °C to 25 °C) revealed that the second-order polynomial regressions gave a slightly better fit due to a slight curvature of thermal relationships, for example, r^2 = 0.99 versus r^2 = 0.93, respectively (U^A_{37} of Sh 1).

4. Discussion

4.1 Isolation and establishment of new strains of alkenone producing haptophytes from Canadian lakes

This study succeeded in isolation and establishment of seven new strains of alkenone-producing haptophytes from Canadian saline lakes. Study basins (Lakes Snakehole, Success and Deadmoose) are located immediately north of the North American freshwater and saline lakes where alkenone-producing microalgae were first identified based on SSU rRNA analysis (Toney et al. 2010, 2012). Interestingly, both Lakes Success and Deadmoose exhibited strong vertical stratification of both temperature and salinity, whereas shallow, but saline, Lake Snakehole seemed to be well-mixed due to vigorous wind at the time of sampling (Supplementary Fig. S2). These differences are consistent with the recent environmental survey of 106 lakes in this region that shows that salinity is the primary control on alkenone presence and concentration, with a secondary influence of stratification

522 (Plancq et al. 2018).

523 Alkenones were most commonly present in deep lakes that
524 ranged in salinity from 2.4 g/L to 44.4 g/L. Although there is no direct
525 experimental evidence on the relationship between such environmental
526 characteristics and the presence of alkenone-producers, the fact that
527 isolation of haptophytes was only successful at sites with hypersaline
528 deep waters suggest that chemical characteristics may be important at
529 some phase of the haptophyte life cycle. In particular, high salinity is
530 often associated with strong anoxia in deep waters (stratified) or
531 sediments (all lakes), consistent with the prior observation that LCAs
532 are associated in lakes with anoxic bottom waters (e.g., Toney et al.
533 2010; Plancq et al., 2018).

534 The presence of flagella and swimming ability in isolates from
535 deep, meromictic Lakes Success and Deadmoose, but not isolates from
536 shallower Lake Snakehole may suggest that access to anoxic water
537 depends in part on the motility of the haptophytes present
538 (Supplementary Fig. S3). On the other hand, non-motile strains might
539 have dry tolerance morphologically, since it was isolated from shore
540 sand. However, as the isolation process employed in this study was just
541 performed once in late September 2014 when the ambient temperature
542 was very low, it is possible that cell growth rates were depressed and
543 inadequate to establish high populations of alkenone-producing

544 microalgae at some sites. Further, as there should be pronounced
545 seasonal variation in haptophyte abundance, we speculate that it may
546 be necessary to collect samples throughout a year from diverse habitats
547 in each lake to fully characterize the presence of alkenone-producing
548 taxa. Thus, the presence of alkenones in sites where viable populations
549 were not isolated most likely reflects differences in the timing of
550 haptophyte growth and alkenone deposition in sediments.

551 The phylogenetic analysis showed that the Canadian lake-
552 isolates can be grouped into three groups, namely Group A including
553 the Lake Snakehole strains near to *I. litoralis* and *I. nuda*, Group B
554 including the Lake Success strains, and Group C including the Lake
555 Deadmoose strains. The LSU rRNA sequences from Lake Snakehole
556 occupy a unique phylogenetic position in the *I. galbana* clade (Fig. 3).
557 Similar relationships were confirmed by the analysis of SSU rRNA
558 sequencing data (Fig. 2). Here, Lake Snakehole strains are positioned
559 near to *Dicrateria* sp. ALGO HAP49 although the *Dicrateria* sp. was
560 renamed to *Isochrysis nuda* after Bendif et al. (2013). The microscopic
561 observations also supported the phylogenetical analyses and showed
562 that the Lake Snakehole strains are different species from *I. galbana*;
563 whereas, the strains from Lake Success and Deadmoose are *I. galbana*.

564

565 *4.2 Characteristics of LCA and alkenoate compositions*

566 *4.2.1 Tetra-unsaturated LCAs and alkenoates*

567 Production of abundant tetra-unsaturated LCAs is considered a
568 common feature of non-calcifying, LCA-producing haptophyte algae
569 that are classified into Groups I and II (Theroux et al., 2010). This
570 pattern appears to also hold for alkenone distributions obtained from
571 either unialgal isolates or environmental samples from a diverse range
572 of lake water salinity, ranging from highly saline brackish and saline
573 inland waters to relatively dilute oligotrophic freshwater systems
574 (Theroux et al., 2010; Longo et al., 2016) (Fig. 2). Among the
575 Isochrysidaceae, both genera *Ruttnera* and *Isochrysis* are known to
576 produce relatively high amounts of tetra-unsaturated LCAs, whereas
577 *Tisochrysis* produces only di- and tri-unsaturated LCAs (Nakamura et
578 al., 2016). Accordingly, the newly isolated Canadian haptophytes
579 strains, such as Sh 1, Sc 2 and Dm 2, were characterized by production
580 of tetra-unsaturated LCAs, especially at lower temperatures. We infer
581 that these results suggest that Sh 1, Sc 2 and Dm 2 are closely related
582 to genus *Isochrysis* and note that this hypothesis is also consistent with
583 phylogenetic trees based on SSU and LSU rRNA sequences (Fig. 2, Fig.
584 3).

585

586 *4.2.2 Double bond position of tri-unsaturated LCA and alkenoate*
587 *isomers*

A small amount of the tri-unsaturated isomer of alkenone ($C_{38:3b}$Et) was detected from newly isolated *Isochrysis* strains Sh 1, Sc 2 and Dm 2, while incomplete chromatographic separation with closely eluting major peak of $C_{38:3a}$Et precludes accurate quantification of $C_{38:3b}$Et (Fig. 5, Supplementary Table S1). Patterns of presence/absence of tri-unsaturated LCAs and alkenoates are considered to serve as chemotaxonomic characteristics for taxonomic assessments of alkenone producers. For example, in general, the LCA profiles of the Group I haptophytes are different from those of the Group II and III haptophytes, including the production of tri-unsaturated alkenone isomers throughout both ethyl and methyl LCAs of the whole range of chain-lengths (Longo et al., 2016). Zheng et al. (2017) further observed *R. lamellosa* LG strain (Group II) and *E. huxleyi* Van 556 (Group III) do not produce tri-unsaturated LCAs, other than a relatively minor amount of $C_{38:3b}$Et. In addition, confirmation of similar patterns (i.e., the sole occurrence of $C_{38:3b}$Et isomer among known tri-unsaturated LCA isomers) in three genetically-different strains of *Isochrysis* reinforces the idea that this pattern is a shared feature for representatives of both *Isochrysis* and *Ruttnera* genera within the Family Isochrysidaceae (Fig. 3).

Relative (%) abundance of $C_{36:3}$FAEE isomers differed between strains closely related to both *I. litoralis* and *I. nuda* (Sh 1) and those

610 more closely related to *I. galbana* (Sc 2, Dm 2). In particular, Sh 1
611 exhibited an α-type isomer of $C_{36:3}$FAEE dominant, while the ß-type
612 isomer was recorded in both Sc 2 and Dm 2 strains (Supplementary
613 Table S1). Interestingly, tri-unsaturated isomers were detected only in
614 $C_{36:3}$FAEE, but not in $C_{36:3}$FAME. This result is in accordance with the
615 sole occurrence of $C_{38:3}$Et isomers in LCAs. These data provide insights
616 on the synthesis of LCAs, and alkenoates in particular, as
617 unsaturation may be specific to a specific chain-length or methyl and
618 ethyl group in the unsaturation at the position of Δ^{28} in the Group II
619 haptophytes.

620 Overall, the isolates from Lakes Snakehole, Success and
621 Deadmoose were from Group II haptophytes. However, while the LCA
622 profile of Sh 1 and Dm 2 showed the $C_{38:3b}$Et isomer, we detected no
623 $C_{38:3b}$Et isomer from the sediment of Lake Snakehole. These results
624 suggest that the presence/absence of tri-unsaturated isomers of
625 alkenoates (Zheng et al., 2016), as well as their relative abundance and
626 response to environmental temperatures, might serve as a
627 chemotaxonomic feature of alkenone-producing haptophyte algae.

628

629 *4.2.3 Unique property of LCAs greater than C_{40} in the Sh 1 strain*

630 The carbon chain length of LCAs in ocean sediments commonly

631 ranges from C_{37} to C_{39}, whereas isolates from lake sediments
632 sometimes contain C_{40} LCAs as minor components. The occurrence of
633 LCAs longer than C_{40} are exceptionally rare as C_{41} and C_{42} LCAs have
634 only been reported from two recent hypersaline lakes in the arid
635 northwestern China (Zhao et al., 2014) and from the Cretaceous
636 marine sediment (Cenomanian black shale, ca. 95 Ma) from western
637 North Atlantic (Deep Sea Drilling Project (DSDP) Site 534; Farrimond
638 et al., 1986).

639 In this context, Sh 1 strain established in this study is the first
640 cultured strain that is characterized as a producer of C_{41} and C_{42} LCAs
641 (Fig. 5, Supplementary Table S1). The molecular phylogenetic tree of
642 LSU and SSU rRNA gene sequences indicate that the Sh 1 strain is
643 most closely related to both *I. litoralis* and *I. nuda* (Fig. 2, Fig. 3).
644 Further investigation on the alkenone profiles of *I. litoralis* and *I. nuda*
645 will be necessary to clarify whether such chemotaxonomic
646 characteristic of > C_{40} LCAs is specific to the Snakehole Lake strain, or
647 whether it is also representative of *I. litoralis* and *I. nuda*. The present
648 results also suggests that the Sh 1 strain might be a candidate taxon
649 responsible for the production of C_{41} and C_{42} LCAs in the hypersaline
650 lakes in the northwestern China reported by Zhao et al. (2014).

651

652 *4.3 Changes in alkenone and alkenoate compositions by growth*
653 *temperature*

654 Similar to previous culture studies, our results show that the
655 entire suite of alkenone homologues, as well as alkenoates, is engaged
656 in the adjustment of alkenone unsaturation and greatly affected by
657 growth temperature of alkenone-producing species (e.g. Prahl et al.,
658 1988; Conte et al., 1998). However, the consistency in the alkenone and
659 alkenoate unsaturation dependence on temperature in the lacustrine
660 isolates is unusual relative to studies from marine isolates, in which a
661 number of other factors have been cited as potentially interfering with
662 the temperature dependence in cultures (e.g., Epstein et al. 1998, 2001;
663 Conte et al. 1995, 1998; Popp et al. 1998; Laws et al. 2001). For
664 example, previous reports in some strains of *E. huxleyi* suggested that
665 alkenone unsaturation degree may also be affected by the difference in
666 physiological conditions/status of cells, such as, the alkenone
667 unsaturation degree increases (i.e. $U_{37}^{K'}$ decreases) more in the
668 stationary growth phase in comparison with the exponential growth
669 phase (Conte et al., 1995, 1998).

670 In this study, isolate cultures were all grown at the same time,
671 under the same conditions, with an experimental design that
672 controlled for temperature as the only variable (i.e., not nutrients, light,
673 water chemistry, etc.). It is worth noting that similar haptophyte

674 species in other lacustrine environments (e.g., Lake George, US, USA)
675 have a similar temperature dependence, based on slopes (Fig. 8) with
676 the isolate cultures (i.e. *I. galbana* CCMP715 and Dm 2). However, in
677 this instance, the y-intercepts observed herein differ from that of
678 culture experiments, which suggests that similar biotic and abiotic
679 conditions likely influence the y-intercept of this correlation as the
680 marine findings, but not the temperature dependency (Toney et al.
681 2010, 2012).

682 The effects of other biotic and abiotic controls on the y-intercept
683 would benefit from further research. Previous studies (Toney et al.
684 2010) show that an *in situ* temperature calibration could be derived for
685 a given lake despite sampling over multiple years, seasons and water
686 depths and that the temperature calibration was valid from 2 °C in
687 more saline bottom waters to 25 °C in surface water. It is possible that
688 the lacustrine algal taxa are better adapted to a variable environment,
689 whereas marine taxa are used to a relatively constant environment. On
690 an annual basis, lakes undergo more extreme variations than oceans,
691 including pH (several units), photon flux (near-surface irradiance to
692 zero at depth), and oxygen (over-saturation to microaerobic conditions
693 over 10-20 m); whereas such variables are more stable in both time and
694 space in many marine systems. While these differences in observed
695 environmental conditions may hold clues to the difference between

reported marine haptophyte cultures versus lacustrine haptophyte cultures, our data suggest that the temperature dependency of the alkenone and alkenoate unsaturation is consistent in both culture and environmental settings for the lake haptophytes.

4.4 Comparison of U^K_{37} calibrations with other species and the lacustrine alkenone profiles: Implications for environmental reconstruction

The U^K_{37}-temperature calibrations obtained for the three newly isolated Canadian haptophyte strains (Sh 1, Sc 2, Dm 2) can be compared with those known previously for other strains of Isochrysidales (Fig. 8). *E. huxleyi* 55a represents a typical planktonic marine producer and serves as a global marine SST calibration (Prahl and Wakeham, 1987). Calibrations of our three Canadian haptophyte cultures most closely resemble to that of *I. galbana* CCMP715 (Theroux et al., 2013) rather than *R. lamellosa* (Nakamura et al., 2014) and *T. lutea* (Nakamura et al., 2016). While similar calibrations were observed at the genus- and species-level, variations within the *Isochrysis* clade become obvious with the comparison of multiple strains enabled by addition of our new cultures. Consequently, future work on *I. litoralis* and *I. nuda* is critical to reinforce the potential species-specific characteristics of strains in the *Isochrysis* clade (i.e. higher temperature sensitivity of Sh 1 strain and production of chain

718 lengths > C_{40}).

719 Application of Sh 1 and Sc 2 calibrations to the U_{37}^{K} index
720 inferred from the sediments of Lakes Snakehole and Success gives
721 modern temperature values of 11.2 °C and 10.3 °C, respectively (Fig. 8).
722 This reconstructed temperature corresponds to water column
723 temperature above the thermocline in Lake Success in autumn
724 (Supplementary Fig. S2). However, all U_{37}^{K} values of strain Dm 2
725 (larger than -0.35) were higher than that of environmental samples
726 obtained from Lake Deadmoose (-0.41 as shown by a horizontal line),
727 which suggests that those values are within range of expected
728 environmental temperatures (Fig. 8). To understand these results, we
729 speculate that other strains which possess the high ability to produce
730 $C_{37:4}$ LCAs may have contributed to the $C_{37:4}$ alkenone pool in
731 sediments. Alternately, we suggest that although the slope of the
732 calibration is defined by temperature dependency, other lake
733 properties, such as nutrients, salinity, etc., may regulate the exact y-
734 intercept. These findings suggest that an *in situ* calibration (e.g.,
735 Toney et al., 2010; 2012) may still be the best approach to capture
736 natural variations in LCA distributions and temperature sensitivity
737 among alkenone producers.

738

739 **5. Conclusions**

740 Seven algal strains were successfully isolated from three salt
741 lakes in Saskatchewan, Canada, and used to establish unialgal
742 cultures. Those strains were classified into the genus *Isochrysis* clade
743 of haptophytes according to SSU and LSU rRNA sequence analysis.
744 One of strains, Sh 1 from Lake Snakehole, was closely related to both *I.*
745 *litoralis* and *I. nuda* according to its phylogenic position and
746 morphological characteristics (i.e., mucoid polysaccharide sheath). The
747 Sh 1 strain exhibited a unique alkenone composition with presence of
748 C_{41} and C_{42} LCAs. This is the first finding of C_{41} and C_{42} LCAs in living
749 haptophytes and the identification of alkenone producer from
750 Canadian saline lakes.

751 The alkenone and alkenoate distributions that characterize the
752 newly isolated haptophyte strains are in good agreement with their
753 taxonomic position as Group II haptophytes and relative other known
754 species. For example, the production of tetra-unsaturated alkenone and
755 alkenoates are common features of the family Isochrysidaceae (except
756 for *T. lutea*), while Sh 1 strain (closely related to both *I. litoralis* and *I.*
757 *nuda*) has a unique alkenone/alkenoate distribution (i.e. > C_{40} LCAs,
758 $C_{36:3}$FAEE compositions) compared to the Sc 2 and Dm 2 strains, which
759 are closely related to *I. galbana*. Comparison of the U_{37}^{K} -growth
760 temperature calibrations among various species also showed that Sh 1,
761 Sc 2 and Dm 2 strains isolated from Lakes Snakehole, Success and

762 Deadmoose were similar to those from *I. galbana* and *R. lamellosa* of
763 the *Isochrysis* clade. Overall, it is hoped that the findings of this study
764 will promote further study on the reconstruction of paleotemperature
765 using alkenone paleothermometer in inland lakes, a task which is
766 substantially less developed in comparison to marine alkenone-
767 paleothermometer studies. Future studies should also include a more
768 comprehensive lake sampling program, to better characterize
769 variability in the timing and spatial extent of alkenone-producing
770 haptophyte populations.

771

772 **Acknowledgments**

773 This study was partly supported by a fund of Core Research for
774 Evolutional Science and Technology in Japan Science and Technology
775 Agency (CREST/JST), Japan, to YS (FY2010–2016) and ERC funding
776 for the ALKENoNE project [Project ID 63776] to JT (FY2015–2020). We
777 thank Ms. M. Atsumi for her technical contribution to the isolation and
778 establishment of newly isolated haptophyte algal strains. We also
779 thank Ms. K. Makino for her technical contribution to extract DNA
780 from Canadian lake-algal isolates and -environmental samples. Field
781 work and preliminary sample preparation funded by an NSERC
782 Canada and Canada Research Chair award to PRL. We are grateful
783 for the constructive comments of two anonymous reviewers, and also

784 for valuable suggestions that helped to improve this manuscript by
785 Editor-in-Chief Dr. John Volkman and Associate Editor Dr. Philip
786 Meyers.

787

788 ***References***

789 Allen M.M., Steiner R.Y., 1968. Growth and division of some
790 unicellular blue-green algae. Journal of General Microbiology 51,
791 199–202.
792 Andersen R.A., Kim J.I., Tittley I., Yoon H.S., 2014. A re-investigation
793 of Chrysotila (Prymnesiophyceae) using material collected from the
794 type locality. Phycologia 53, 463–473.
795 Bendif E.M., Probert I., Schroeder D.C., de Vargas C., 2013. On the
796 description of *Tisochrysis lutea* gen. nov. sp. nov. and *Isochrysis*
797 *nuda* sp. nov. in the Isochrysidales, and the transfer of *Dicrateria* to
798 the Prymnesiales (Haptophyta). Journal of Applied Phycology 25,
799 1763–1776.
800 Bendle J., Rosell-Melé A., Ziveri P., 2005. Variability of unusual
801 distributions of alkenones in the surface waters of the Nordic seas.
802 Paleoceanography 20, PA2001.
803 Boon J.J., F.W., Van der Meer P.W.J., Schuyl de Leeuw J.W., Schenck
804 P.A., 1978. Organic geochemical analysis of core samples from site
805 362, Walvis Ridge, DSDP Leg 40, Deep Sea Drilling Project Initial

Reports 40, 627–637.

Brassell S.C., Comet P.A., Eglinton G., Isaacson P.J., McEvoy J., Maxwell J.R., Thomson I.D., Tibbets P.J.C., Volkman J.K., 1980. Preliminary lipid analyses of Sections 440A- 7-6, 440B-3-5, 440B-8-4, 440B-68-2, and 436-11-4: Legs 56 and 57, Deep Sea Drilling Project Initial Reports 56 & 57, 1367–1390.

Brassell S.C., Eglinton G., Marlowe I.T., Pflaumann U., Sarnthein M., 1986. Molecular stratigraphy: a new tool for climatic assessment. Nature 320, 129–133.

Brassell S.C., 1993. Applications of biomarkers for delineating marine paleoclimatic fluctuations during the Pleistocene, In: Engel, M.H., Macko, S.A. (Eds.), Organic Geochemistry: Principles and Applications. Plenum Press, New York, pp. 699–738.

Chu G., Sun Q., Li S., Zheng M., Jia X., Lu C., Liu J., Liu T., 2005. Long-chain alkenone distributions and temperature dependence in lacustrine surface sediments from China. Geochimica et Cosmochimica Acta 69, 4985–5003.

Chu G., Sun Q., Wang X., Liu M., Lin Y., Xie M., Shang W., Liu J., 2012. Seasonal temperature variability during the past 1600 years recorded in historical documents and varved lake sediment profiles from northeastern China. The Holocene 22, 785–792.

Conte M.H., Thompson A., Eglinton G., 1995. Lipid biomarker diversity in the coccolithophorid Emiliania huxleyi

(Prymnesiophyceae) and related species Gephyrocapsa oceanica. Journal of Phycology. 31, 272–282.

Conte M.H., Thompson A., Lesley D., Harris R.P., 1998. Genetic and physiological influences on the alkenone/alkenoate versus growth temperature relationship in Emiliania huxleyi and Gephyrocapsa oceanica. Geochimica et Cosmochimica Acta 62, 51–68.

Coolen M.J.L., 2004. Combined DNA and lipid analyses of sediments reveal changes in Holocene haptophyte and diatom populations in an Antarctic lake. Earth and Planetary Science Letters 223, 225–239.

Coolen M.J.L., Saenz, J.P., Giosan, L., Trowbridge, N.Y., Dimitrov, P., Dimitrov, D., Eglinton, T.I., 2009. DNA and lipid molecular stratigraphic records of haptophyte succession in the Black Sea during the Holocene. Earth and Planetary Science Letters 284, 610–621.

Cranwell P.A., 1985. Long-chain unsaturated ketones in recent lacustrine sediments. Geochimica et Cosmochimica Acta 49, 1545–1551.

D'Andrea W.J., Lage M., Martiny J.B.H., Laatsch A.D., Amaral-Zettler L.A., Sogin M.L., Huang Y., 2006. Alkenone producers inferred from well-preserved 18S rDNA in Greenland lake sediments. Journal of Geophysical Research 111, G03013.

D'Andrea W.J., Huang Y., Fritz S.C., Anderson N.J., 2011. Abrupt

852 Holocene climate change as an important factor for human
853 migration in West Greenland. Proceedings of the National Academy
854 of Sciences of the United States of America 108, 9765–9769.
855 Danbara A., Shiraiwa Y., 1999. The Requirement of Selenium for the
856 Growth of Marine Coccolithophorids, *Emiliania huxleyi*,
857 *Gephyrocapsa oceanica* and *Helladosphaera* sp. (Prymnesiophyceae).
858 Plant Cell Physiology 40, 762–766.
859 De Leeuw J.W., Van der Meer F.W., Rijpstra W.I.C., Schenck P.A.,
860 1980. On the occurrence and structural identification of long chain
861 unsaturated ketones and hydrocarbons in sediments. Physics and
862 Chemistry of the Earth 30, 211–217.
863 Dillon J.T., Longo W.M., Zhang Y., Torozo R., Huang Y., 2016.
864 Identification of double-bond positions in isomeric alkenones from a
865 lacustrine haptophyte. Rapid Communications in Mass
866 Spectrometry 30, 112–118.
867 Epstein B.L., D'Hondt S., Hargraves P.E., 2001. The possible metabolic
868 role of C_{37} alkenones in *Emiliania huxley*i. Organic Geochemistry 32,
869 867–875.
870 Epstein B.L., D'Hondt S., Quinn J.G., Zhang J., Hargraves P.E., 1998.
871 An effect of dissolved nutrient concentrations on alkenone-based
872 temperature estimates. Paleoceanography 13, 126.
873 Farrimond P., Eglinton G. and Brassell S.C., 1986. Alkenones in
874 Cretaceous black shales, Blake-Bahama Basin, western North

875 Atlantic, Organic Geochemistry 10, 897–903.
876 Galtier N., Gouy M., Gautier C., 1996. SEAVIEW and PHYLO_WIN:
877 two graphic tools for sequence alignment and molecular phylogeny.
878 Bioinformatics 12, 543–548.
879 Hou J., Huang Y., Zhao J., Liu Z., Colman S., An Z., 2016. Large
880 Holocene summer temperature oscillations and impact on the
881 peopling of the northeastern Tibetan Plateau. Geophysical Research
882 Letters 43, 1323–1330.
883 Katoh K., Standley D.M., 2013. MAFFT multiple sequence alignment
884 software version 7: Improvements in performance and usability.
885 Molecular Biology and Evolution 30, 772–780.
886 Laws E.A., Popp B.N., Bidigare R.R., Riebesell U., Burkhardt S., 2001.
887 Controls on the molecular distribution and carbon isotopic
888 composition of alkenones in certain haptophyte algae. Geochemistry,
889 Geophysics, Geosystems 2, 2000GC000057.
890 Liu H., Probert I., Uitz J., Claustre H., Aris-Brosou S., Frada M., Not
891 F., Vargas de C., 2009. Extreme diversity in noncalcifying
892 haptophytes explains a major pigment paradox in open oceans.
893 Proceedings of the National Academy of Sciences of the United
894 States of America 106, 12803–12808.
895 Longo W.M., Dillon J.T., Tarozo R., Salacup J.M., Huang Y., 2013.
896 Unprecedented separation of long chain alkenones from gas
897 chromatography with a poly (trifluoropropylmethylsiloxane)

898 stationary phase. Organic Geochemistry 65, 94–102.
899 Longo W.M., Theroux S., Giblin A.E., Zheng Y., Dillon J.T., Huang Y.,
900 2016. Temperature calibration and phylogenetically distinct
901 distributions for freshwater alkenones: Evidence from northern
902 Alaskan lakes. Geochimica et Cosmochimica Acta 180, 177–196.
903 Marlowe, I.T., Brassell, S.C., Eglinton, G., Green, J.C., 1984. Long
904 chain unsaturated ketones and esters in living algae and marine
905 sediments. Organic Geochemistry 6, 135-141.
906 Medlin L.K., Saez A.G., Young J.R., 2008. A molecular clock for
907 coccolithophores and implications for selectivity of phytoplankton
908 extinctions across the K/T boundary. Marine Micropaleontology 67,
909 69–86.
910 Nakamura H., Sawada K., Araie H., Suzuki I., Shiraiwa Y., 2014. Long
911 chain alkenes, alkenones and alkenoates produced by the
912 haptophyte alga *Chrysotila lamellosa* CCMP1307 isolated from a
913 salt marsh. Organic Geochemistry 66, 90–97.
914 Nakamura H., Sawada K., Araie H., Shiratori T., Ishida K., Suzuki I.,
915 Shiraiwa Y., 2016. Composition of long chain alkenones and
916 alkenoates as a function of growth temperature in marine
917 haptophyte Tisochrysis lutea. Organic Geochemistry 99, 78–89.
918 Nguyen L.T., Schmidt H.A., von Haeseler A, Minh B.Q., 2015. IQ-
919 TREE: A fast and effective stochastic algorithm for estimating
920 maximum likelihood phylogenies. Molecular Biology and Evolution

921 32, 268–274
922 Ono M., Sawada K., Shiraiwa Y., Kubota M., 2012. Changes in
923 alkenone and alkenoate distributions during acclimatization to
924 salinity change in Isochrysis galbana: Implication for alkenone-
925 based paleosalinity and paleothermometry. Geochemical Journal 46,
926 235–247.
927 Pearson E.J., Juggins S., Farrimond P., 2008. Distribution and
928 significance of long-chain alkenones as salinity and temperature
929 indicators in Spanish saline lake sediments. Geochimica et
930 Cosmochimica Acta 72, 4035–4046.
931 Pham S.V., Leavitt P.R., McGowan S., Wissel B., Wassenaar L., 2009.
932 Spatial and temporal variability of prairie lake hydrology as
933 revealed using stable isotopes of hydrogen and oxygen. Limnology
934 and Oceanography 54, 101–118.
935 Plancq, J., Cavazzin, B., Juggins, S., Haig, H.A., Leavitt, P.R., Toney,
936 J.L., 2018. Assessing environmental controls on the distribution of
937 long-chain alkenones in the Canadian Prairies. Organic
938 Geochemistry. 117, 43-55.
939 Popp B.N., Kenig F., Wakeham S.G., Laws E.A., Bidigare R.R., 1998.
940 Does growth rate affect ketone unsaturation and intracellular
941 carbon isotopic variability in *Emiliania huxleyi*? Paleoceanography
942 13, 35–41.
943 Prahl F.G., Wakeham S.G., 1987. Calibration of unsaturation patterns

944 in long-chain ketone compositions for palaeotemperature
945 assessment. Nature 330, 367–369.
946 Prahl F.G., Muehlhausen L.A., Zahnle D.L., 1988. Further evaluation
947 of long-chain alkenones as indicators of paleoceanographic
948 conditions. Geochimica et Cosmochimica Acta 52, 2303–2310.
949 Randlett M.È., Coolen M.J.L., Stockhecke M., Pickarski N., Litt T.,
950 Balkema C., Kwiecien O., Tomonaga Y., Wehrli B., Schubert C.J.,
951 2014. Alkenone distribution in Lake Van sediment over the last 270
952 ka: influence of temperature and haptophyte species composition.
953 Quaternary Science Reviews 104, 53–62.
954 Ronquist F., Teslenko M., von der Mark P., Ayres D.L., Darlig A.,
955 Höhna S., Larget B., Liu L., Suchard M.A., Huelsenbeck J.P., 2012.
956 MrBayes 3.2: efficient Bayesian phylogenetic inference and model
957 choice across a large model space. Systematic Biology 61, 539–542.
958 Rontani J.F., Beker B., Volkman J.K.. 2004. Long-chain alkenones and
959 related compounds in the benthic haptophyte Chrysotila lamellosa
960 Anand HAP 17. Phytochemistry 65, 117–126.
961 Sawada K., Handa N., Shiraiwa Y., Danbara A., Montani S., 1996.
962 Long-chain alkenones and alkyl alkenoates in the coastal and
963 pelagic sediments of the northwest North Pacific, with special
964 reference to the reconstruction of *Emiliania huxleyi* and
965 *Gephyrocapsa oceanica* ratios. Organic Geochemistry 24, 751–764.
966 Schulz H.M., Schöner A., Emeis K.C., 2000. Long-chain alkenone

patterns in the Baltic sea-an ocean-freshwater transition. Geochimica et Cosmochimica Acta 64, 469–477.

Schwab V.F., Sachs J.P., 2011. Hydrogen isotopes in individual alkenones from the Chesapeake Bay estuary. Geochimica et Cosmochimica Acta 75, 7552–7565.

Sun Q., Chu G., Liu G., Li S., Wang X., 2007. Calibration of alkenone unsaturation index with growth temperature for a lacustrine species, *Chrysotila lamellosa* (Haptophyceae). Organic Geochemistry 38, 1226–1234.

Theroux S., D'Andrea W.J., Toney J., Amaral-Zettler L., Huang, Y., 2010. Phylogenetic diversity and evolutionary relatedness of alkenone-producing haptophyte algae in lakes: Implications for continental paleotemperature reconstructions. Earth and Planetary Science Letters 300, 311–320.

Theroux S., Toney J., Amaral-Zettler L., Huang Y., 2013. Production and temperature sensitivity of long chain alkenones in the cultured haptophyte *Pseudoisochrysis paradoxa*. Organic Geochemistry 62, 68–73.

Toney J.L., Huang Y., Fritz S.C., Baker P.A., Grimm E., Nyren P., 2010. Climatic and environmental controls on the occurrence and distributions of long chain alkenones in lakes of the interior United States. Geochimica et Cosmochimica Acta 74, 1563–1578.

Toney J.L., Leavitt P.R., Huang Y., 2011. Alkenones are common in

990 prairie lakes of interior Canada. Organic Geochemistry 42, 707–712.
991 Toney J.L., Theroux S., Andersen R.A., Coleman A., Amaral-Zettler L.,
992 Huang, Y., 2012. Culturing of the first 37:4 predominant lacustrine
993 haptophyte: Geochemical, biochemical, and genetic implications.
994 Geochimica et Cosmochimica Acta 78, 51–64.
995 Versteegh G.J.M., Riegman R., de Leeuw J.W., Jansen J.H.F.F., 2001.
996 $U_{37}^{K'}$ values for Isochrysis galbana as a function of culture
997 temperature, light intensity and nutrient concentrations. Organic
998 Geochemistry 32, 785–794.
999 Volkman J.K., Eglinton G., Corner E.D.S., Forsberg T.E.V., 1980a.
1000 Long-chain alkenes and alkenones in the marine coccolithophorid
1001 Emiliania huxleyi. Phytochemistry 19, 2619–2622.
1002 Volkman J.K., Eglinton G., Corner E.D.S., Sargent J.R., 1980b. Novel
1003 unsaturated straight-chain C_{37}–C_{39} methyl and ethyl ketones in
1004 marine sediments and coccolithophore *Emiliania huxleyi*, In:
1005 Douglas A.G. and Maxwell J.R. (Ed.), Advances in Organic
1006 Geochemistry 1979, Pergamon Press, Oxford, pp. 219–227.
1007 Volkman J.K., Burton H.R., Everitt D.A., Allen D.I., 1988. Pigment and
1008 lipid compositions of algal and bacterial communities in Ace Lake,
1009 Vestfold Hills, Antarctica, In: Ferris, J.M., Burton, H.R., Johnstone,
1010 G.W., Bayly, I.A.E. (Eds.), Biology of the Vestfold Hills, Antarctica.
1011 Developments in Hydrobiology 34. Springer, Dordrecht, pp. 41–57.
1012 Watanabe M.M., Kawachi M., Hiroki M., Kasai F., 2000. NIES

1013 Collection List of Strains, Microalgae and Protozoa, Sixth Ed.
1014 Microbial Culture Collections, National Institute for Environmental
1015 Studies, Tsukuba, 159 pp.
1016 Yabuki A., Inagaki Y., Ishida K.-I., 2010. *Palpitomonas bilix* gen. et sp.
1017 nov.: A novel deep-branching heterotroph possibly related to
1018 Archaeplastida or Hacrobia. Protist 161, 523–538.
1019 Zhao J., An C., Longo W.M., Dillon J.T., Zhao Y., Shi C., Chen Y.,
1020 Huang Y., 2014. Occurrence of extended chain length C_{41} and C_{42}
1021 alkenones in hypersaline lakes. Organic Geochemistry 75, 48–53.
1022 Zheng Y., Huang Y., Andersen R.A., Amaral-Zettler L.A., 2016.
1023 Excluding the di-unsaturated alkenone in the U_{37}^{K} index strengthens
1024 temperature correlation for the common lacustrine and brackish-
1025 water haptophytes. Geochimica et Cosmochimica Acta 175, 36–46.
1026 Zheng Y., Tarozo R., Huang Y., 2017. Optimizing chromatographic
1027 resolution for simultaneous quantification of long chain alkenones,
1028 alkenoates and their double bond positional isomers. Organic
1029 Geochemistry 111, 136–143.
1030 Zink K.G., Leythaeuser D., Melkonian M., Schwark L., 2001.
1031 Temperature dependency of long-chain alkenone distributions in
1032 recent to fossil limnic sediments and in lake waters. Geochimica et
1033 Cosmochimica Acta 65, 253–265.
1034
1035

Table captions:

Table 1 List of Canadian lakes where the isolations of microalgae and LSU rRNA were performed from lake water and sediments with corresponding environmental data for the lakes.

[a]Y and N indicate yes (positive) and no (negative), respectively.

[b]The results of alkenone analysis are also listed according to literature (Toney et al. 2010).

Table 2 List of seven algal strains established as unialgal cultures (**A**) and six environmental samples of which haptophyte marker genes were successfully amplified (**B**) accompanied with the names of lakes, materials used for isolation, salinity, culture medium used for algal isolation, and the Genebank accession numbers of SSU and LSU rRNAs registered in Genebank obtained by amplification.

[a]The information of salinity/medium indicates the salinity of MA-ESM medium used for establishing unialgal strains and cultivation of algal mixture from environmental samples, respectively.

Table 3 Correlation equations between the LCAs and alkenoate unsaturation indices and the growth temperature.

[a]These data were obtained from laboratory cultured alkenone-producing haptophyte strains of Sh 1, Sc 2 and Dm 2 which had been isolated from three Canadian salt lakes of Snakehole, Success and Deadmoose, respectively.

[b]The correlation equations were obtained from data calculation by the linear and second-order polynomial regressions with correlation coefficient (R2). For graphs, see Fig. 6 and 7 on the alkenone and alkenoate unsaturation indices including related parameters, respectively.

Figure legends:

Fig. 1 Light micrographs of seven algal strains established as unialgal cultures after the isolation of algae from three Canadian saline lakes. **A** and **B**, two strains isolated from Lake Snakehole (Sh), named as Sh 1 and Sh 2; **C** and **D**, two strains isolated from Lake Success (Sc), named as Sc 1 and Sc 2; **E**–**G**, three strains isolated from Lake Deadmoose (Dm), named as Dm 1, Dm 2 and Dm 3. Scale bar in each photo is 50 µm.

Fig. 2 Maximum likelihood tree of the three Canadian lakes haptophyte strains constructed by the analysis of SSU rRNA gene

1077 sequences. Six samples analyzed are prepared from strains Sh 1, Sh
1078 2, Sc 1, Sc 2 and Dm 2, Dm 3 which were isolated from Lake
1079 Snakehole, Success and Deadmoose, respectively. The values of
1080 bootstrap percentage (BP) and Bayesian posterior probability (BPP)
1081 are expressed as BP/BPP on each note by selecting values with only
1082 BP >P50% and BPP>P0.5.

1083

1084 **Fig. 3** Maximum likelihood tree of the three Canadian lakes
1085 haptophyte strains constructed by the analysis of D1–D2 region of
1086 LSU rRNA gene sequences. For the values of BP/, see Fig. 2.
1087 Symbols: ●, samples prepared from the seven isolated haptophyte
1088 strains of Sh 1 and Sh 2, Sc 1 and Sc 2, Dm 1, Dm 2 and Dm 3
1089 isolated from Lakes Snakehole (Sh), Success (Sc) and Deadmoose
1090 (Dm), respectively; ▲, six environmental samples expressed as Sh
1091 E1 and Sh E2, Sc E1, Sc E2 and Sc E3, and Ws E1 extracted from
1092 the algal mixture cultivated from environmental samples of three
1093 Canadian high salt lakes of Snakehole (Sh), Success (Sc) and
1094 Waldsea (Ws), respectively.

1095

1096 **Fig. 4** Growth curves of three haptophyte strains established as
1097 unialgal cultures of Sh 1 (isolated from Lake Snakehole), Sc 2

(isolated from Lake Success) and Dm 2 (isolated from Lake Deadmoose) grown under different temperatures. Comparison of growth curves among various temperatures at 5 (×), 10 (◆), 15 (■), 20 (▲) and 25 °C (●) in the strains Sh 1 (**A**), Sc 2 (**B**) and Dm 2 (**C**). Comparison of growth curves among the strains of Sh 1 (○), Sc 2 (△) and Dm 2 (□) grown at 5 (**D**), 10 (**E**), 15 (**F**), 20 (**G**) and 25 °C (**H**). The y-axes of graphs were logarithmic scales. Error bars denote the standard deviation of triplicate cultures.

Fig. 5 Partial GC–FID chromatograms of LCAs and alkenoates extracted from the lake sediments (rows **A** and **B**) and the isolated haptophyte strains of Sh 1, Sc 2 and Dm 2 (rows **C** and **D**) from the three Canadian saline lakes of Lake Snakehole, Success and Deadmoose, respectively. Samples **B** and **D** were prepared by removing alkyl alkenoates after saponification of alkenone fractions **A** and **C**, respectively. Peak assignments: 1. $C_{36:4}$FAME, 2. $C_{36:3}$FAME, 3: $C_{36:2}$FAME, 4. $C_{36:4}$FAEE, 5. $C_{36:3a}$FAEE, 6. $C_{36:3b}$FAEE, 7. $C_{36:2}$FAEE, 8. $C_{37:4}$Me, 9. $C_{37:3}$Me, 10. $C_{37:2}$Me, 11. $C_{38:4}$Et, 12. $C_{38:3a}$Et, 13. $C_{38:3b}$Et, 14. $C_{38:2}$Et, 15. $C_{38:3}$Me, 16. $C_{38:2}$Me, 17. $C_{39:3}$Et, 18. $C_{39:2}$Et, 19. $C_{39:3}$Me, 20. $C_{39:2}$Me, 21. $C_{40:3}$Et, 22. $C_{40:2}$Et, 23. $C_{41:3}$Me, 24. $C_{41:2}$Me, 25. $C_{42:3}$Et, 26. $C_{42:2}$Et. *: unidentified peaks.

1120

1121 **Fig. 6** Relationship between growth temperature and the alkenone
1122 unsaturation indices in the three established haptophyte strains
1123 isolated from Canadian saline lakes, namely Sh 1, Sc 2 and Dm 2
1124 isolated from Lakes Snakehole, Success, and Deadmoose,
1125 respectively. Correlation equations (y) are shown in each figure with
1126 correlation coefficients (R^2). The definitions of various alkenone and
1127 alkenoate unsaturation indices are shown in the panel.

1128

1129 **Fig. 7** Relationship between growth temperature and the alkenoate
1130 unsaturation indices U_{37}^{A} and U_{38}^{A}, the ratio of isomeric alkenoates
1131 (RIA_{38}) and the ratio of methyl to ethyl alkenoates (A_{37}/A_{38}) in the
1132 three established haptophyte strains isolated from Canadian saline
1133 lakes, namely Sh 1, Sc 2 and Dm 2. Correlation equations (y) are
1134 shown in each figure with correlation coefficients (R^2). For the
1135 definitions of the unsaturation indices and the other parameters, see
1136 the inset (in the right bottom) of Fig. 6.

1137

1138 **Fig. 8** Comparison of the culture-based U_{37}^{K}-temperature calibrations
1139 among the newly obtained strains Sh 1, Sc 2 and Dm 2 (classified
1140 into Isochrysidaceae, Haptophyta) and those of the other species

reported in literatures. For reference, U_{37}^{K}-values in environmental samples extracted from sediments of Lakes Snakehole, Success and Deadmoose are indicated by colored horizontal lines at the values of -0.38, -0.41 and -0.30, respectively. Symbols: **Sh 1** (▲ with a red line), strain Sh 1 isolated from Lake Snakehole; **Sc 2** (□ with a dashed line), strain Sc 2 isolated from Lake Success**; Dm 2** (○ with a dotted line), strain Dm 2 isolated Lake Deadmoose; **a**, *E. huxleyi* 55a (Noëlaerhabdaceae), representative of typical planktonic marine species (Prahl and Wakeham, 1987); **b**, *T. lutea* CCMP 463 (Nakamura et al. 2016); **c**, *T. lutea* NIES-2590 (Nakamura et al. 2016); **d**, *I. galbana* CCMP 715 (Nakamura et al. 2014). **e**, *R. lamellosa* CCMP 1307 (Nakamura et al. 2014); **Lake George**, data from *in-situ* calibration of the Lake George (Toney et al., 2012).

Figure 1

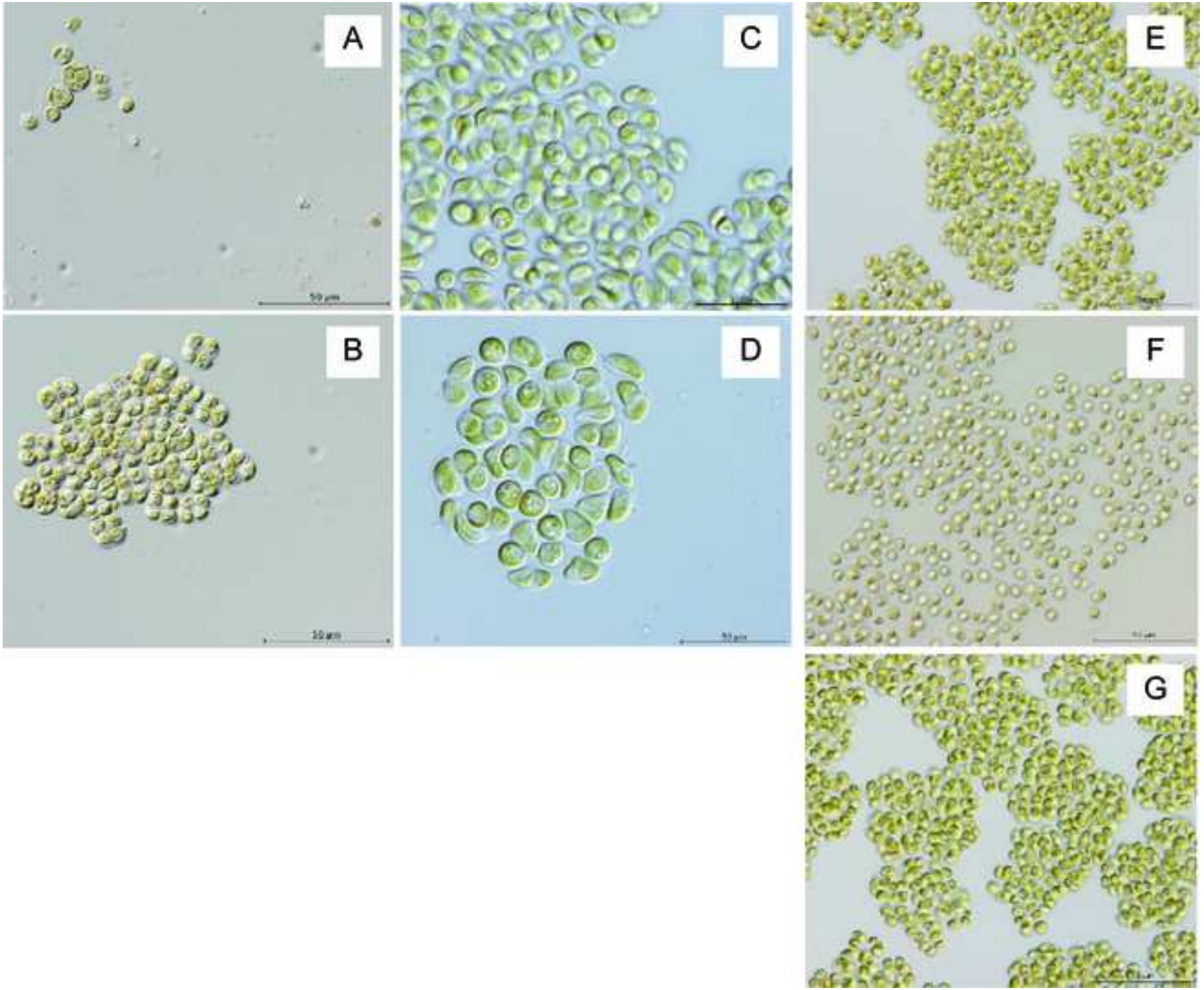

Figure 2

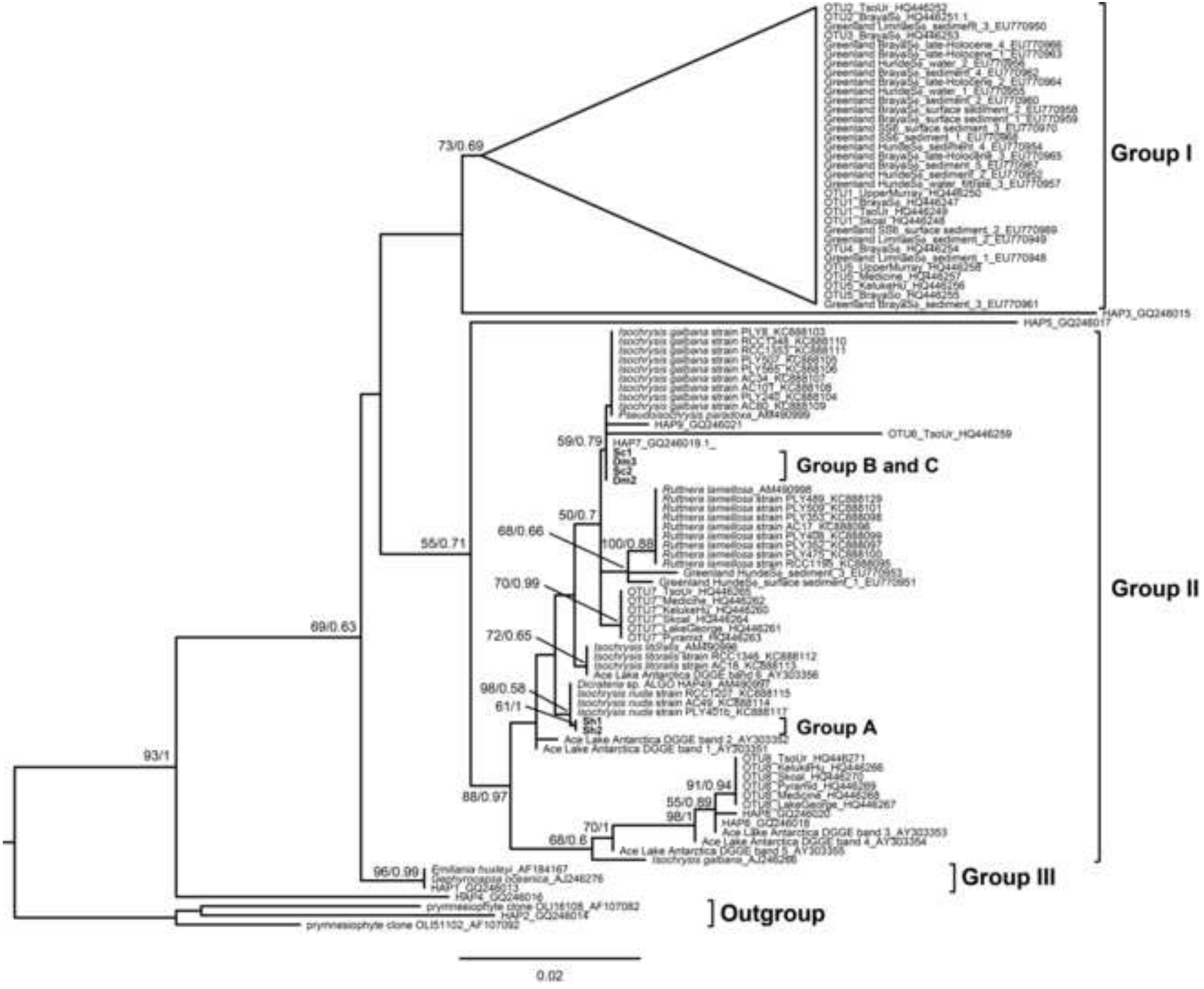
Group I
Group II
Group B and C
Group A
Group III
Outgroup
73/0.69
59/0.79
50/0.7
68/0.66
55/0.71
100/0.88
70/0.99
69/0.63
72/0.65
98/0.58
61/1
93/1
88/0.97
91/0.94
55/0.89
98/1
70/1
68/0.6
96/0.99
0.02

Figure 3

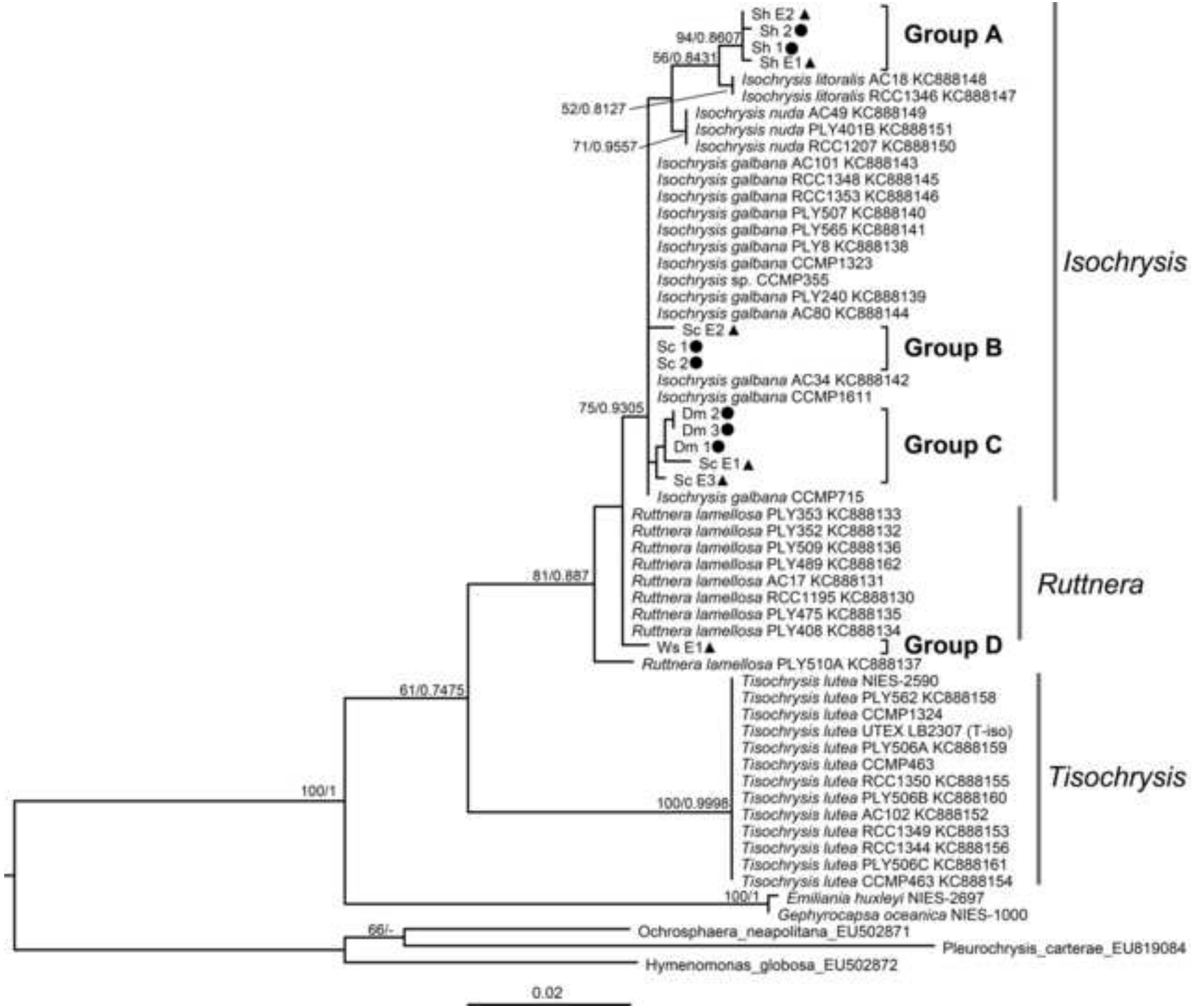
Sh E2 ▲
Sh 2 ●
Sh 1 ●
Sh E1 ▲
94/0.8607
56/0.8431
Group A
Isochrysis litoralis AC18 KC888148
Isochrysis litoralis RCC1346 KC888147
52/0.8127
Isochrysis nuda AC49 KC888149
Isochrysis nuda PLY401B KC888151
71/0.9557
Isochrysis nuda RCC1207 KC888150
Isochrysis galbana AC101 KC888143
Isochrysis galbana RCC1348 KC888145
Isochrysis galbana RCC1353 KC888146
Isochrysis galbana PLY507 KC888140
Isochrysis galbana PLY565 KC888141
Isochrysis galbana PLY8 KC888138
Isochrysis galbana CCMP1323
Isochrysis sp. CCMP355
Isochrysis galbana PLY240 KC888139
Isochrysis galbana AC80 KC888144
Isochrysis
Sc E2 ▲
Sc 1 ●
Sc 2 ●
Group B
Isochrysis galbana AC34 KC888142
Isochrysis galbana CCMP1611
75/0.9305
Dm 2 ●
Dm 3 ●
Dm 1 ●
Sc E1 ▲
Sc E3 ▲
Group C
Isochrysis galbana CCMP715
Ruttnera lamellosa PLY353 KC888133
Ruttnera lamellosa PLY352 KC888132
Ruttnera lamellosa PLY509 KC888136
Ruttnera lamellosa PLY489 KC888162
81/0.887
Ruttnera lamellosa AC17 KC888131
Ruttnera lamellosa RCC1195 KC888130
Ruttnera lamellosa PLY475 KC888135
Ruttnera lamellosa PLY408 KC888134
Ruttnera
Ws E1 ▲
Group D
Ruttnera lamellosa PLY510A KC888137
Tisochrysis lutea NIES-2590
Tisochrysis lutea PLY562 KC888158
Tisochrysis lutea CCMP1324
Tisochrysis lutea UTEX LB2307 (T-iso)
Tisochrysis lutea PLY506A KC888159
Tisochrysis lutea CCMP463
Tisochrysis lutea RCC1350 KC888155
Tisochrysis lutea PLY506B KC888160
Tisochrysis lutea AC102 KC888152
Tisochrysis lutea RCC1349 KC888153
Tisochrysis lutea RCC1344 KC888156
Tisochrysis lutea PLY506C KC888161
Tisochrysis lutea CCMP463 KC888154
Tisochrysis
61/0.7475
100/1
100/0.9996
100/1
Emiliania huxleyi NIES-2697
Gephyrocapsa oceanica NIES-1000
66/-
Ochrosphaera_neapolitana_EU502871
Pleurochrysis_carterae_EU819084
Hymenomonas_globosa_EU502872
0.02

Figure 4

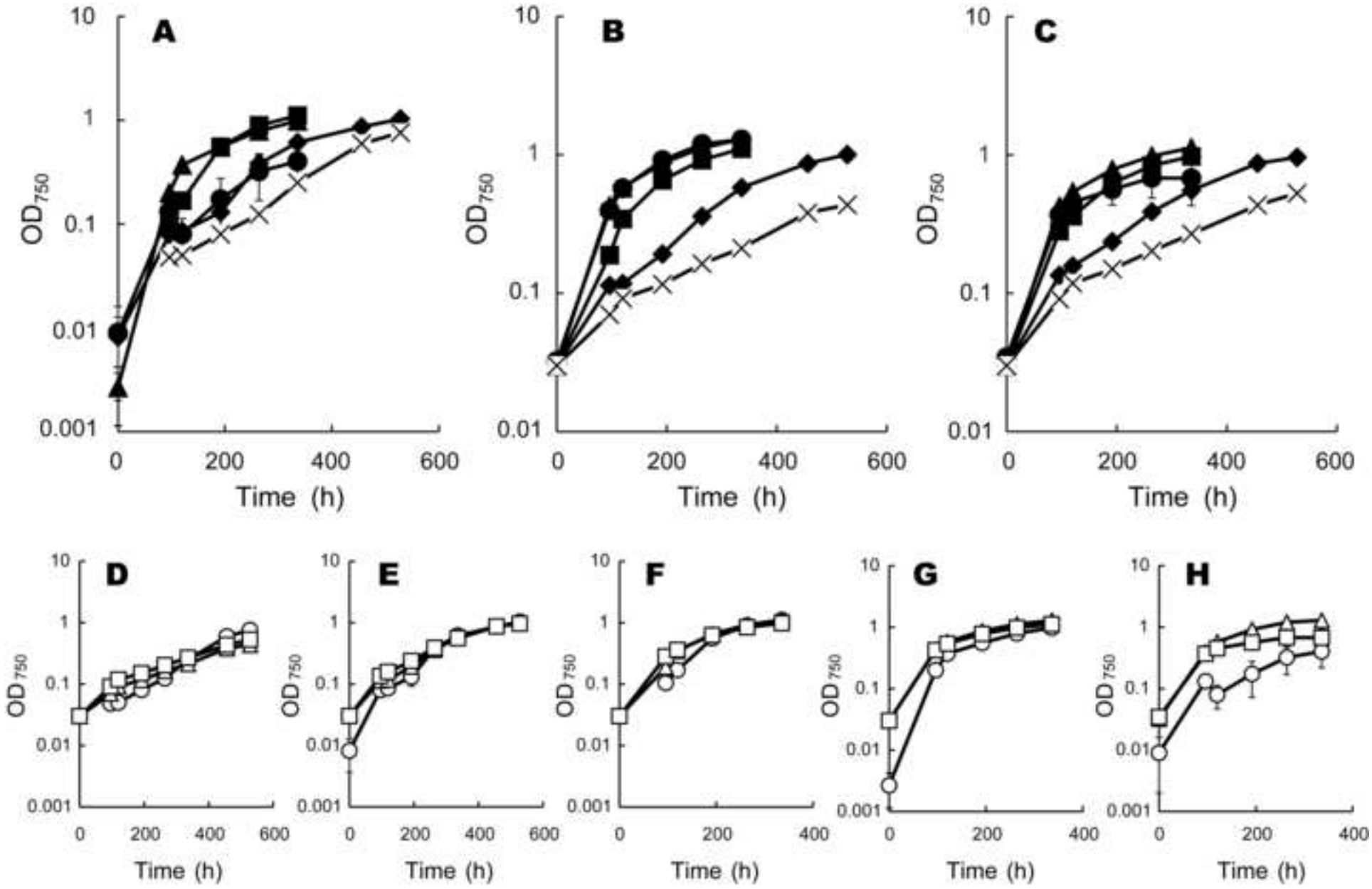

Figure 5

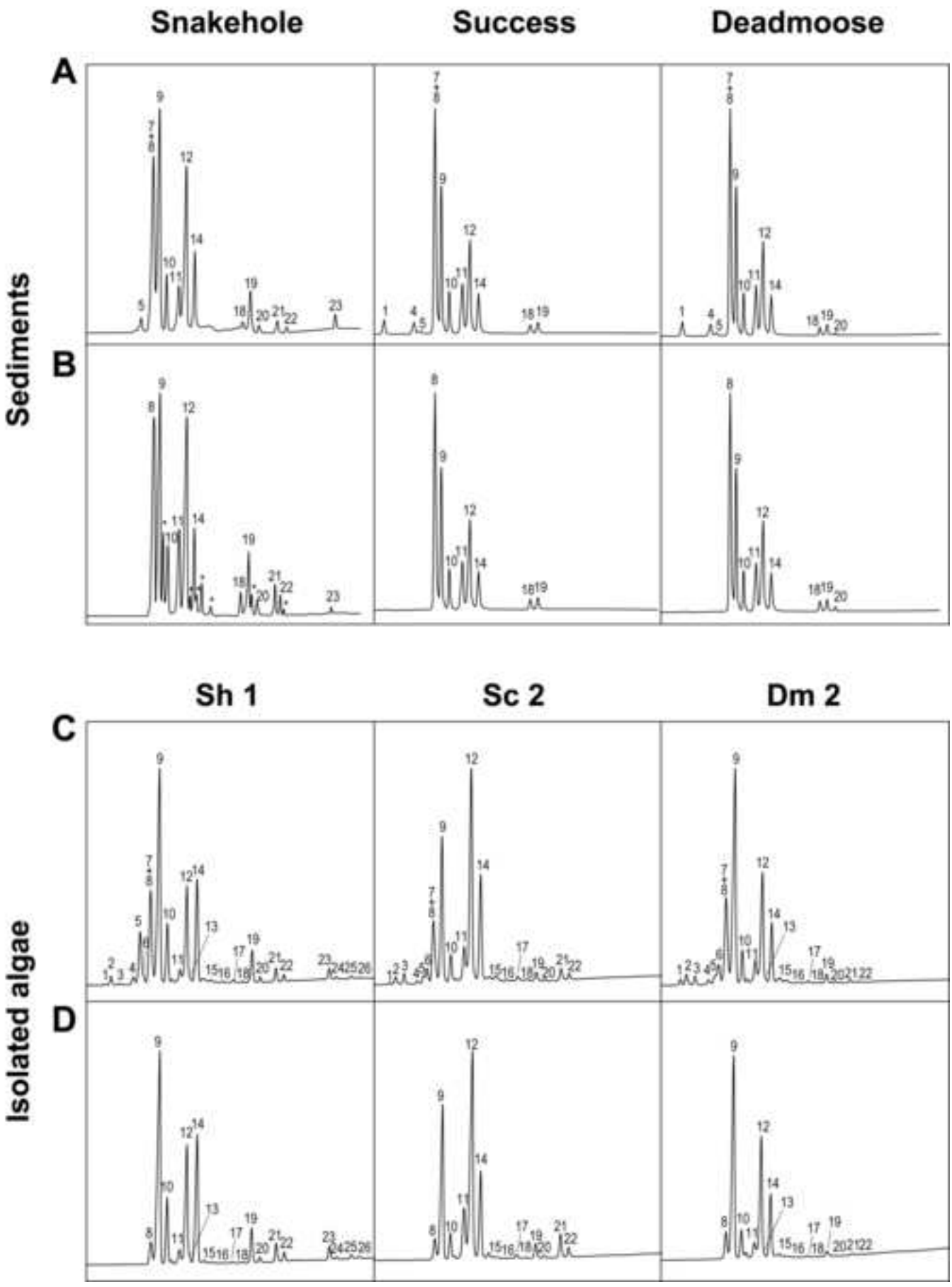
Snakehole
Success
Deadmoose
A
B
Sediments
Sh 1
Sc 2
Dm 2
C
D
Isolated algae

Figure 6

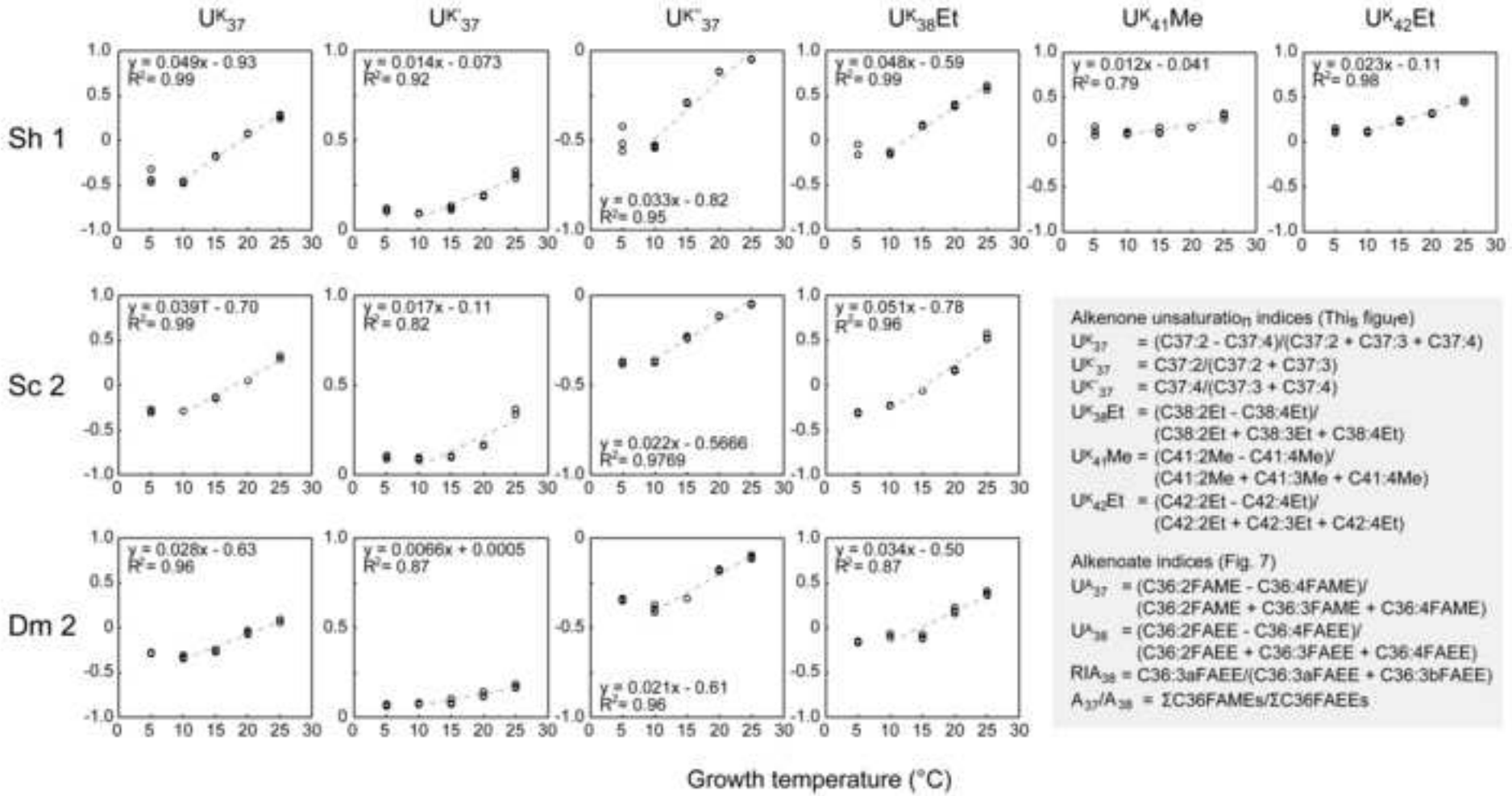

Alkenone unsaturation indices (This figure)

U^{K}_{37} = (C37:2 - C37:4)/(C37:2 + C37:3 + C37:4)

$U^{K'}_{37}$ = C37:2/(C37:2 + C37:3)

$U^{K''}_{37}$ = C37:4/(C37:3 + C37:4)

$U^{K}_{38}Et$ = (C38:2Et - C38:4Et)/(C38:2Et + C38:3Et + C38:4Et)

$U^{K}_{41}Me$ = (C41:2Me - C41:4Me)/(C41:2Me + C41:3Me + C41:4Me)

$U^{K}_{42}Et$ = (C42:2Et - C42:4Et)/(C42:2Et + C42:3Et + C42:4Et)

Alkenoate indices (Fig. 7)

U^{A}_{37} = (C36:2FAME - C36:4FAME)/(C36:2FAME + C36:3FAME + C36:4FAME)

U^{A}_{38} = (C36:2FAEE - C36:4FAEE)/(C36:2FAEE + C36:3FAEE + C36:4FAEE)

RIA_{38} = C36:3aFAEE/(C36:3aFAEE + C36:3bFAEE)

A_{37}/A_{38} = ΣC36FAMEs/ΣC36FAEEs

Figure 7

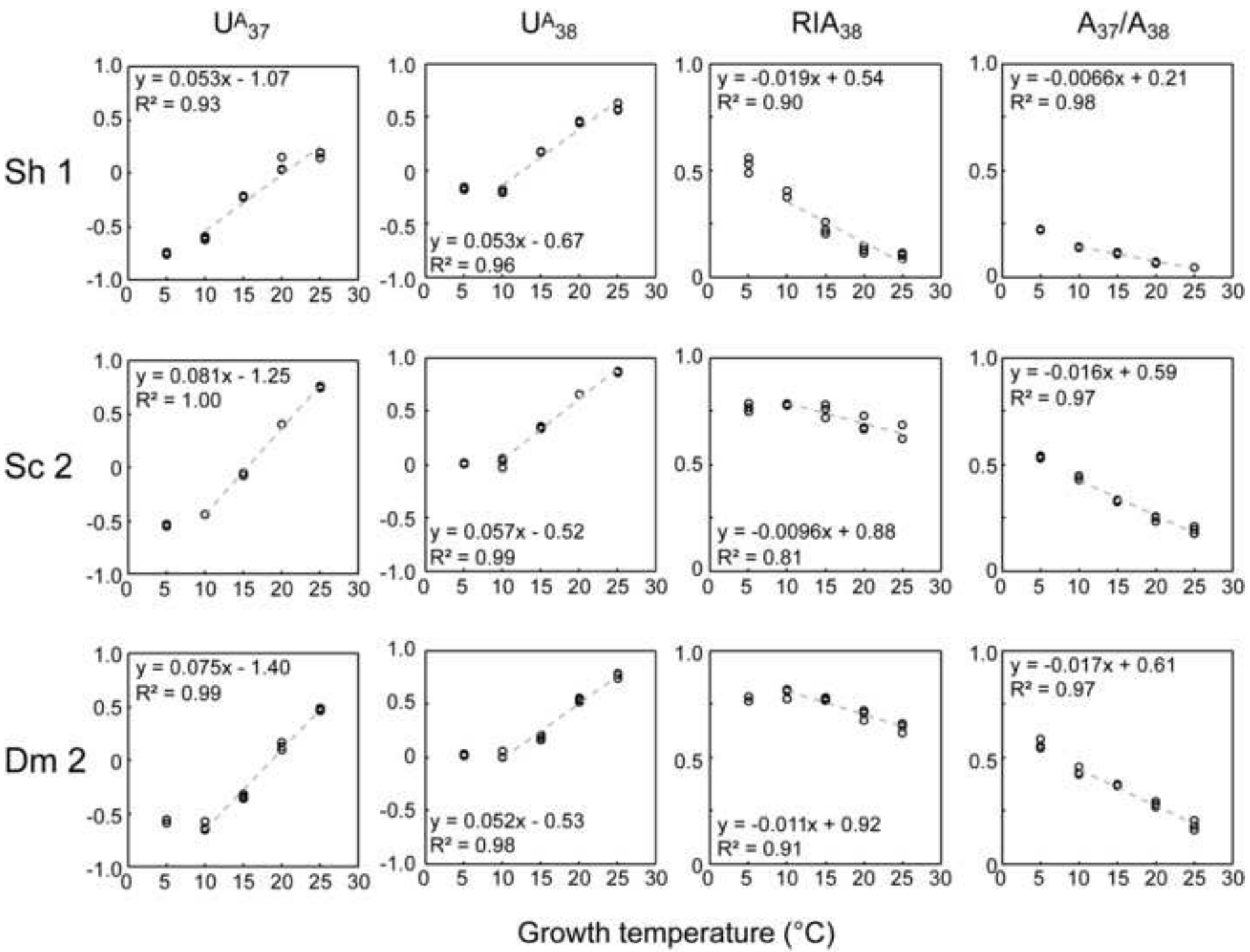
UA_{37}
UA_{38}
RIA_{38}
A_{37}/A_{38}
Sh 1
Sc 2
Dm 2
y = 0.053x - 1.07
R² = 0.93
y = 0.053x - 0.67
R² = 0.96
y = -0.019x + 0.54
R² = 0.90
y = -0.0066x + 0.21
R² = 0.98
y = 0.081x - 1.25
R² = 1.00
y = 0.057x - 0.52
R² = 0.99
y = -0.0096x + 0.88
R² = 0.81
y = -0.016x + 0.59
R² = 0.97
y = 0.075x - 1.40
R² = 0.99
y = 0.052x - 0.53
R² = 0.98
y = -0.011x + 0.92
R² = 0.91
y = -0.017x + 0.61
R² = 0.97
Growth temperature (°C)

Figure 8

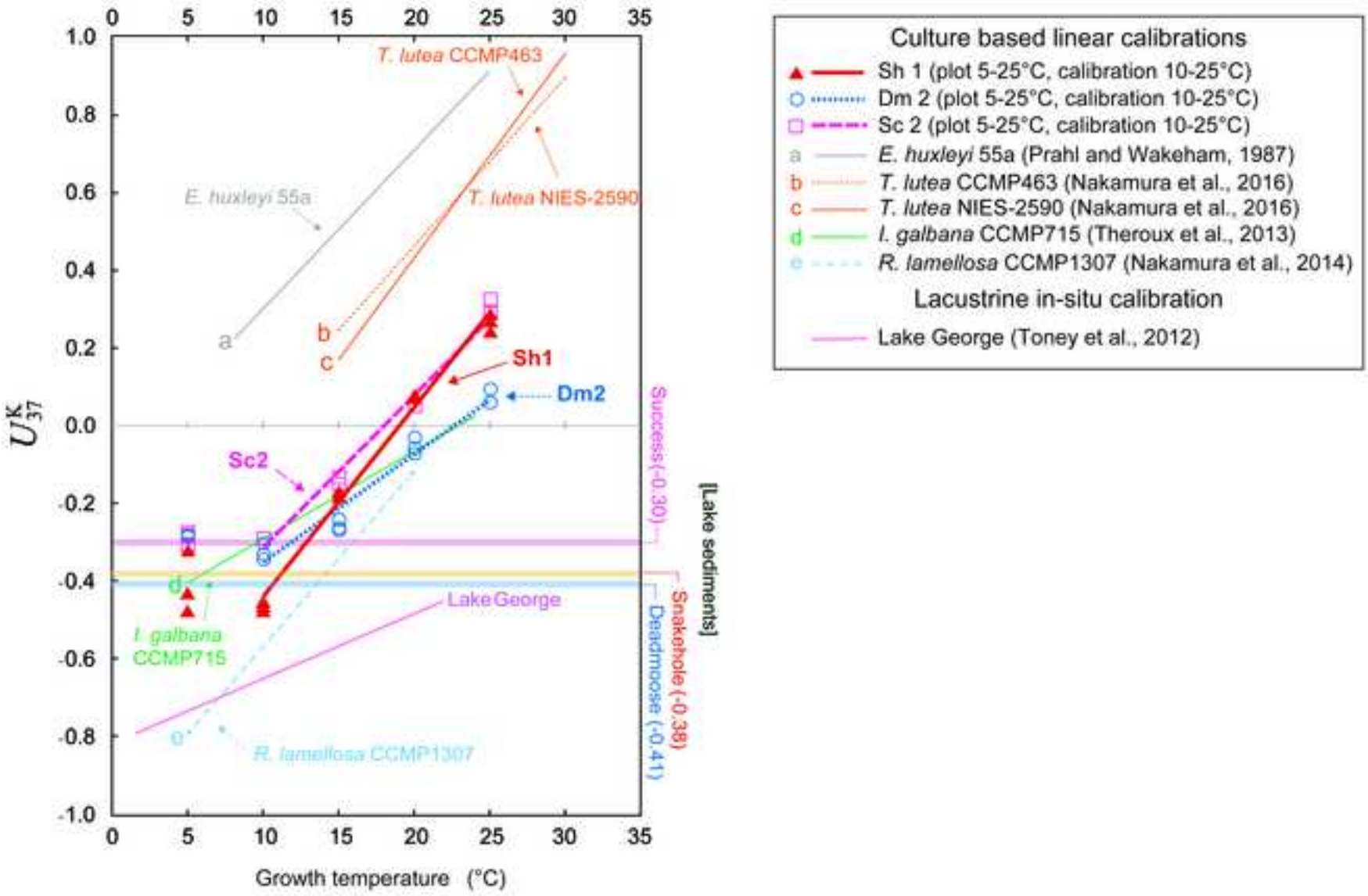
Culture based linear calibrations
Sh 1 (plot 5-25°C, calibration 10-25°C)
Dm 2 (plot 5-25°C, calibration 10-25°C)
Sc 2 (plot 5-25°C, calibration 10-25°C)
a E. huxleyi 55a (Prahl and Wakeham, 1987)
b T. lutea CCMP463 (Nakamura et al., 2016)
c T. lutea NIES-2590 (Nakamura et al., 2016)
d I. galbana CCMP715 (Theroux et al., 2013)
e R. lamellosa CCMP1307 (Nakamura et al., 2014)
Lacustrine in-situ calibration
Lake George (Toney et al., 2012)
T. lutea CCMP463
E. huxleyi 55a
T. lutea NIES-2590
Sh1
Dm2
Sc2
I. galbana CCMP715
Lake George
R. lamellosa CCMP1307
Success (-0.30)
Snakehole (-0.38)
Deadmoose (-0.41)
[Lake sediments]
Growth temperature (°C)

Table 1

Table 1. List of Canadian lakes where the isolations of microalgae and LSU rRNA were performed from lake water and sediments with corresponding environmental data for the lakes.

Lake Name	Isolation[a]	LSU rRNA amplification[i]	Salinity (g L^{-1})	pH	Alkenone parameters in the sediments[b]								
					Alkenones (µg g^{-1}sed)	Alkenoates (µg g^{-1}sed)	% Alkenones	% Alkenoates	%$C_{37:4}$	U^{K}_{37}	$U^{K'}_{37}$	U^{K}_{38}	C_{37}/C_{38}
Antelope	N	N	7.87	9.40	66.39	6.46	91.13	8.87	45.67	-0.66	0.17	-0.09	5.57
Snakehole	Y	Y	50.21	8.96	8.06	0.23	97.25	2.75	27.73	-0.38	0.13	0.07	1.97
Success	Y	Y	34.97	8.62	5.59	0.21	96.42	3.58	19.94	-0.30	0.28	-0.06	1.09
Fishing	N	N	1.31	9.17	4.90	0.90	84.49	15.51	27.10	-0.60	0.23	-0.42	1.32
Humboldt	N	N	0.84	9.13	2.34	0.59	79.77	20.23	41.64	-0.53	0.06	-0.14	7.05
Waldsea	N	Y	12.82	8.45	180.87	14.44	92.61	7.39	38.26	-0.68	0.17	-0.18	1.35
Deadmoose	Y	N	12.27	8.87	31.60	7.61	80.58	19.42	33.00	-0.41	0.27	-0.18	1.73
Charron	N	N	4.9	10.55	150.05	6.83	95.65	4.35	46.64	-0.58	0.19	0.04	3.53
Rabbit	N	N	4.23	9.21	8.95	0.98	90.17	9.83	50.28	-0.64	0.19	-0.01	4.59
Redberry	N	N	8.61	9.09	357.70	9.00	97.54	2.46	49.18	-0.67	0.18	-0.26	3.20

Table 2

Table 2. List of seven algal strains established as unialgal cultures (A) and six environmental samples of which haptophyte marker genes were successfully amplified (B) accompanied with the names of lakes, materials used for isolation, salinity, culture medium used for algal isolation, and the Genebank accession numbers of SSU and LSU rRNAs registered in Genebank obtained by amplification.

A	Isolated Strain Name	Isolated lake	Sample used for isolation	Salinity / Medium[a]	Genbank accession number	
					SSU rRNA	LSU rRNA
	Sh 1	Snakehole	Shore sand	40‰ MA-ESM	LC322312	LC322318
	Sh 2	Snakehole	Shore sand	40‰ MA-ESM	LC322313	LC322319
	Sc 1	Success	Sediment	30‰ MA-ESM	LC322314	LC322320
	Sc 2	Success	Sediment	30‰ MA-ESM	LC322315	LC322321
	Dm 1	Deadmoose	Sediment	40‰ MA-ESM	-	LC322322
	Dm 2	Deadmoose	Sediment	40‰ MA-ESM	LC322316	LC322323
	Dm 3	Deadmoose	Sediment	40‰ MA-ESM	LC322317	LC322324
B	Sample name of amplified DNA	Sample lake	Sample used for amplification	Salinity / Medium[a]	Genbank accession number	
					SSU rRNA	LSU rRNA
	Sh E1	Snakehole	Surface water	40‰ MA-ESM	-	LC322325
	Sh E2	Snakehole	Shore sand	40‰ MA-ESM	-	LC322326
	Sc E1	Success	Sediment	40‰ MA-ESM	-	LC322327
	Sc E2	Success	Sediment	40‰ MA-ESM	-	LC322328
	Sc E3	Success	Sediment	40‰ MA-ESM	-	LC322329
	Ws E1	Waldsea	PlanktonNet	10‰ MA-ESM	-	LC322330

Table 3

Table 3. Correlation equations between the LCAs and alkenoate unsaturation indices and the growth temperature.

Unsaturation indices[a]	Temperature range and type of fit	Regressions vs. temperature (T)[b]					
		Sh 1	R^2	Sc 2	R^2	Dm 2	R^2
Alkenone indices							
U^{K}_{37}	10–25; polynom.	$-0.001T^2 + 0.085T - 1.21$	1.00	$0.001T^2 + 0.0046T - 0.43$	1.00	$0.0006T^2 + 0.0086T - 0.48$	0.97
	10–25; linear	$0.049T - 0.93$	0.99	$0.039T - 0.70$	0.99	$0.028T - 0.63$	0.96
$U^{K'}_{37}$	10–25; polynom.	$0.0009T^2 - 0.016T + 0.17$	0.99	$0.0017T^2 - 0.043T + 0.35$	0.99	$0.0004T^2 - 0.0068T + 0.11$	0.93
	10–25; linear	$0.014T - 0.073$	0.92	$0.017T - 0.11$	0.82	$0.0066T - 0.0005$	0.87
$U^{K''}_{37}$	10–25; polynom.	$-0.0017T^2 + 0.094T - 1.30$	1.00	$-0.0007T^2 + 0.046T - 0.76$	1.00	$0.0002T^2 + 0.0145T - 0.57$	0.96
	10–25; linear	$0.033T - 0.82$	0.95	$0.022T - 0.57$	0.98	$0.021T - 0.61$	0.96
$U^{K}_{38}Et$	10–25; polynom.	$-0.001T^2 + 0.082T - 0.86$	1.00	$0.0021T^2 - 0.022T - 0.21$	1.00	$0.0021T^2 - 0.038T + 0.06$	0.94
	10–25; linear	$0.048T - 0.59$	0.99	$0.051T - 0.78$	0.96	$0.0342T - 0.50$	0.87
$U^{K}_{41}Me$	10–25; polynom.	$0.0011T^2 - 0.026T + 0.25$	0.91				
	10–25; linear	$0.012T - 0.041$	0.79				
$U^{K}_{42}Et$	10–25; polynom.	$0.0002T^2 + 0.014T - 0.047$	0.98				
	10–25; linear	$0.023T - 0.11$	0.98				
Alkenoate indices							
U^{A}_{37}	10–25; polynom.	$-0.0029T^2 + 0.15T - 1.85$	0.99	$-0.0003T^2 + 0.091T - 1.33$	1.00	$0.0006T^2 + 0.053T - 1.23$	0.99
	10–25; linear	$0.053T - 1.07$	0.93	$0.081T - 1.25$	1.00	$0.075T - 1.41$	0.99
U^{A}_{38}	10–25; polynom.	$-0.0024T^2 + 0.14T - 1.32$	1.00	$-0.0012T^2 + 0.099T - 0.85$	1.00	$0.0006T^2 + 0.030T - 0.36$	0.98
	10–25; linear	$0.053T - 0.67$	0.96	$0.057T - 0.52$	0.99	$0.052T - 0.53$	0.98
RIA_{38}	10–25; polynom.	$0.0013T^2 - 0.064T + 0.90$	0.98	$-0.0002T^2 - 0.0026T + 0.83$	0.82	$-0.0003T^2 + 0.0004T + 0.83$	0.92
	10–25; linear	$-0.019T + 0.54$	0.90	$-0.0096T + 0.88$	0.81	$-0.011T + 0.92$	0.91
A_{37}/A_{38}	10–25; polynom.	$4.3\times10^{-5}T^2 + 0.0081T + 0.22$	0.98	$0.0006T^2 - 0.036T + 0.75$	0.99	$-0.0003T^2 - 0.0054T + 0.52$	0.98
	10–25; linear	$-0.0066T + 0.21$	0.98	$-0.016T + 0.59$	0.97	$-0.017T + 0.61$	0.97